Pergamon

Geochimica et Cosmochimica Acta, Vol. 59, No. 16, pp. 3301–3325, 1995

0016-7037/95 $9.50 + .00

0016-7037(95)00128-9

The fluvial geochemistry and denudation rate of the Guayana Shield in Venezuela, Colombia, and Brazil

J. M. EDMOND,[1] M. R. PALMER,[1,*] C. I. MEASURES,[1,†] B. GRANT,[1] and R. F. STALLARD[2,‡]

[1]Department of Earth, Atmospheric and Planetary Sciences, Massachusetts Institute of Technology, E34-201, Cambridge, MA 02139, USA
[2]Department of Geological and Geophysical Sciences, Guyot Hall, Princeton University, Princeton, NJ 08544, USA

(*Received June* 17, 1994; *accepted in revised form May* 19, 1995)

Abstract—The Guayana Shield is composed of Early to Mid-Precambrian igneous and metamorphic basement rocks with a quartzitic platform cover. The complete absence of limestones and evaporites allows a clear chemical expression in the stream data of the primary weathering of the basement in a humid tropical environment. Total erosion rates are extremely slow, ~10 m/m.y., with equal contributions from the dissolved and suspended loads. However, the former is largely silica with ratios of Si to total cation equivalents [Si:TZ$^+$] ranging to in excess of three. Weathering is "complete" to kaolinite and gibbsite, i.e., the environment is one of active laterisation with a penetration rate of the weathering front into the fresh substrate about twice the denudation rate. In basins of relatively homogeneous lithology, Rb/Sr isochrons constructed from the river data agree with the whole-rock ages from the drainages; thus, all the common, refractory, Rb-containing minerals (K-feldspar, mica) are completely dissolved. The thick, lateritic regolith that is accumulating as a result of this intense weathering is a common relict feature on other Southern Hemisphere Shields. In the absence of active tectonics or greatly accelerated mechanical erosion, the weathering rates of these basement rocks must be quite insensitive to environmental change.

1. INTRODUCTION

The fluxes to the ocean of material derived from the chemical and mechanical weathering of the continents are central components of the global geochemical budget. As such, their estimation has attracted sustained attention since the earliest development of the Earth Sciences (see Garrels and Mackenzie (1971) and Holland (1978) for discussion). In addition, global rates of chemical weathering are a major determinant on atmospheric pCO_2 levels and have been the focus of extensive model simulations (e.g., Berner et al., 1983; Berner, 1994). However, there are many difficulties involved.

Historically, most attention has been paid to the processes of mechanical erosion and deposition since these contribute to the geologic record in an explicit fashion, whereas the dissolved yield is usually dispersed and homogenized ocean-wide before eventual removal. Estimates of regional mechanical erosion rates over geological timescales can be made if the resulting detrital sediments can be located quantitatively (Menard, 1961; Richter et al., 1992). This may depend on seismic exploration and proof by drilling and, even in tectonically quiescent areas, is an uncertain process. Data are often proprietary and subject to misinterpretation especially in offshore areas. The resolved timescales can be long with respect to tectonic events in the drainage, with the result that interpretation of the data in terms of elevation, climate, etc. is ambiguous.

Contemporary weathering rates can be determined, in principle, by monitoring the discharge and the dissolved and suspended load of streams (Milliman and Meade, 1983; Meade, 1988). However, anthropogenic perturbations in a drainage can increase the mechanical erosion rate by over a factor of ten (Meade, 1969; Trimble, 1977; Gong and Xu, 1987). The accompanying effects on the dissolved load are not well known but are probably substantial. Industrial activity also results in contamination, particularly of the dissolved load, on a regional or even a continental scale, e.g., for sulfate. Routine stream monitoring is rarely carried out for scientific purposes but instead to develop a predictive hydrologic database for engineering use in the construction of dams, bridges, ports, and irrigation schemes (Nordin, 1985). Hence, most of the available data is, in fact, from impacted areas. In many tectonically active regimes, where erosion rates are very rapid, the streams are small and have unstable hydrographs (Nordin and Meade, 1980). Infrequent events of short duration can provide most of the sediment transport; thus long, densely sampled time-series are required to obtain accurate estimates. More subtle effects of sediment storage within basins have been recognized for many years (Gilbert, 1917; Meade et al., 1990b), but often are not appreciated by scientific users of the data (Schumm, 1963). In mountainous or high latitude regions glaciation may have produced large amounts of easily erodible morainic debris leading to spuriously high values for the contemporary rate of mechanical denudation (Meade, 1988). Since sediment storage increases the time available for reaction and since glacial erosion, particularly of massive igneous and metamorphic rocks, greatly increases the surface area available for chemical attack, it is probable that the dissolved load transport is also increased by these processes, perhaps markedly (Newton et al., 1987).

Geochemical models of the evolution of atmospheric pCO_2 over geologic time require precise information on the relationships between climate (greenhouse temperature), lithology, and relief, and chemical weathering rates (Berner et al.,

* *Present address:* Department of Geology, University of Bristol, Bristol, BF8 1RJ, UK.
† *Present address:* Department of Oceanography, University of Hawaii, Honolulu, HI, 96822, USA.
‡ *Present address:* Water Resources Division, USGS, Denver, CO 80225, USA.

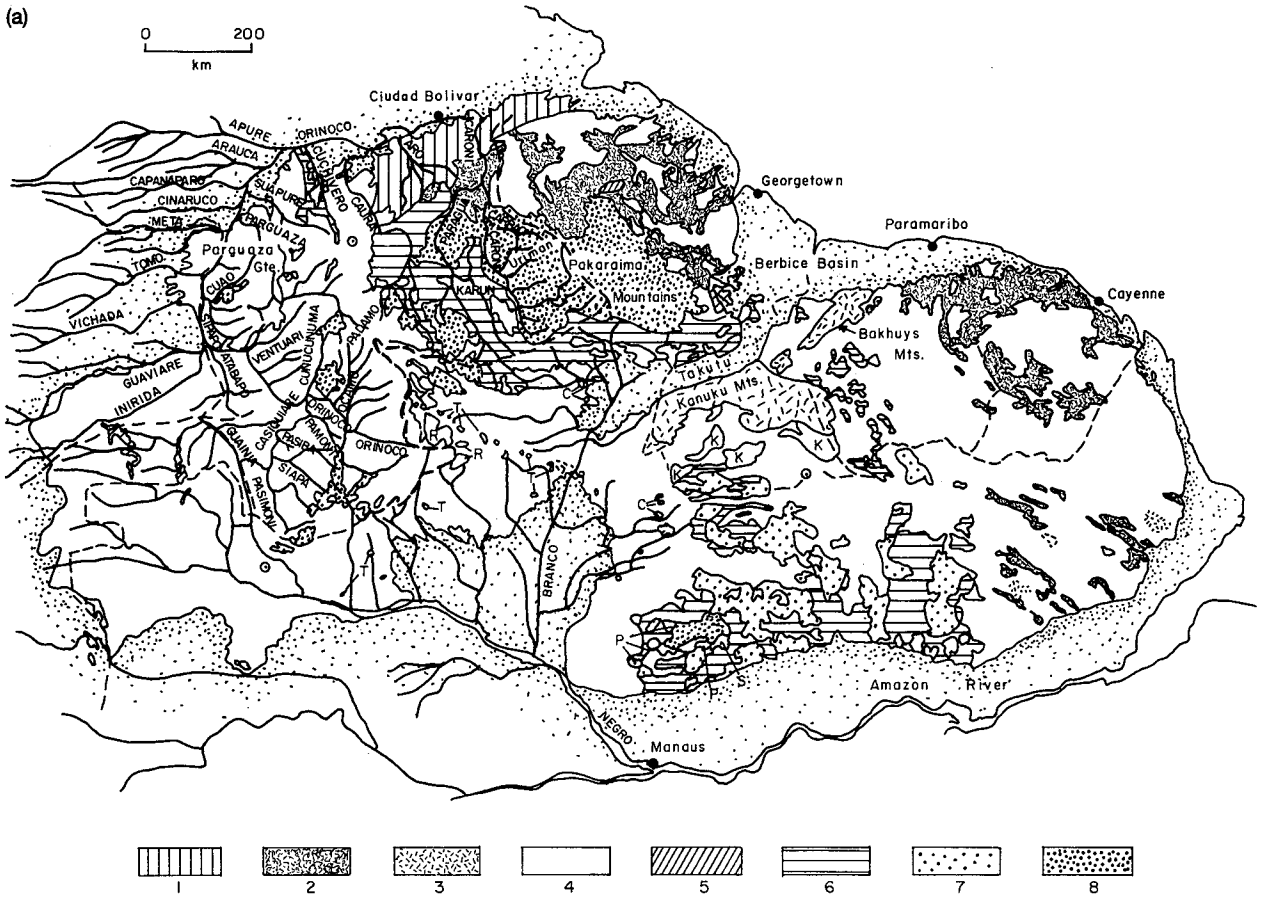

FIG. 1. (a) Geologic map of the Guayana Shield in Venezuela, Colombia, Brazil and the Guayanas (after Gibbs and Barron, 1983). Key: 1—Imataca Complex; 2—Greenstone Belts; 3—high-grade Trans-Amazonian metamorphic rocks; 4—undifferentiated Proterozoic rocks; 5—Middle Proterozoic pre-Uatuma sedimentary rocks; 6—Uatuma Supergroup volcanics; 7—Granitoid rocks of the Uatuma; 8—Roraima Group. (b) Topographic map of that portion of the Guayana Shield within the drainage of the Orinoco. The Orinoco watershed boundary is indicated by the dashed line.

1983; Berner, 1994). In the absence of such information the present generation of models parameterise this relationship in a very simple fashion. Systematic studies of weathering processes as a function of environment are required if valid simulations of the long-term variations in atmospheric pCO_2 are to be achieved.

Based on current understanding there are several criteria that have to be met if valid estimates of contemporary weathering and denudation rates are to be obtained from the monitoring of stream discharges. The drainage should be lithologically homogeneous so that parameters for specific rock types can be obtained. It should also be sufficiently large that, under the prevailing climatic conditions, the hydrograph is stable, i.e., it is not subject to domination by individual localized storms. The landscape should be free from anthropogenic perturbations and recent glacial activity. It goes without saying that the stream should be accurately gauged. The density of sampling and the statistical requirements for the length of the record can only be decided based on the characteristics of the particular system under investigation.

A recent hydrologic and geochemical reconnaissance of the Guayana Shield in Venezuela and Colombia has shown that the above criteria are reasonably well met in this region. As the last unexploited continental Shield area in the world (Fig. 1a,b), this craton is expected to host major mineral resources (Sidder, 1990; Sidder and Martinez, 1990). Giant lateritic Fe and bauxite deposits are already being mined and there is rapidly accelerating working of Au, diamond, and Sn placers. The elevated regions have a substantial potential for hydroelectric power development. At present, however, there are only two dams on the Shield, the major Guri complex and the much smaller Macagua both on the lower Caroni, where most of the mining and refining activity is also concentrated. There is some grain farming in the savanna areas of the Aro and Ventuari. The rest of the Shield is almost completely unaffected by human activities save for those of the small native population.

The present project is also intended to provide a scientific and engineering basis for the anticipated development of the Orinoco Basin. The work reported here derives from a systematic survey of the discharge and dissolved and suspended load transport of the major streams in the Basin carried out under the auspices of the Proyecto Orinoco-Apure of the Ministerio del Ambiente y de los Recursos Naturales Renovables

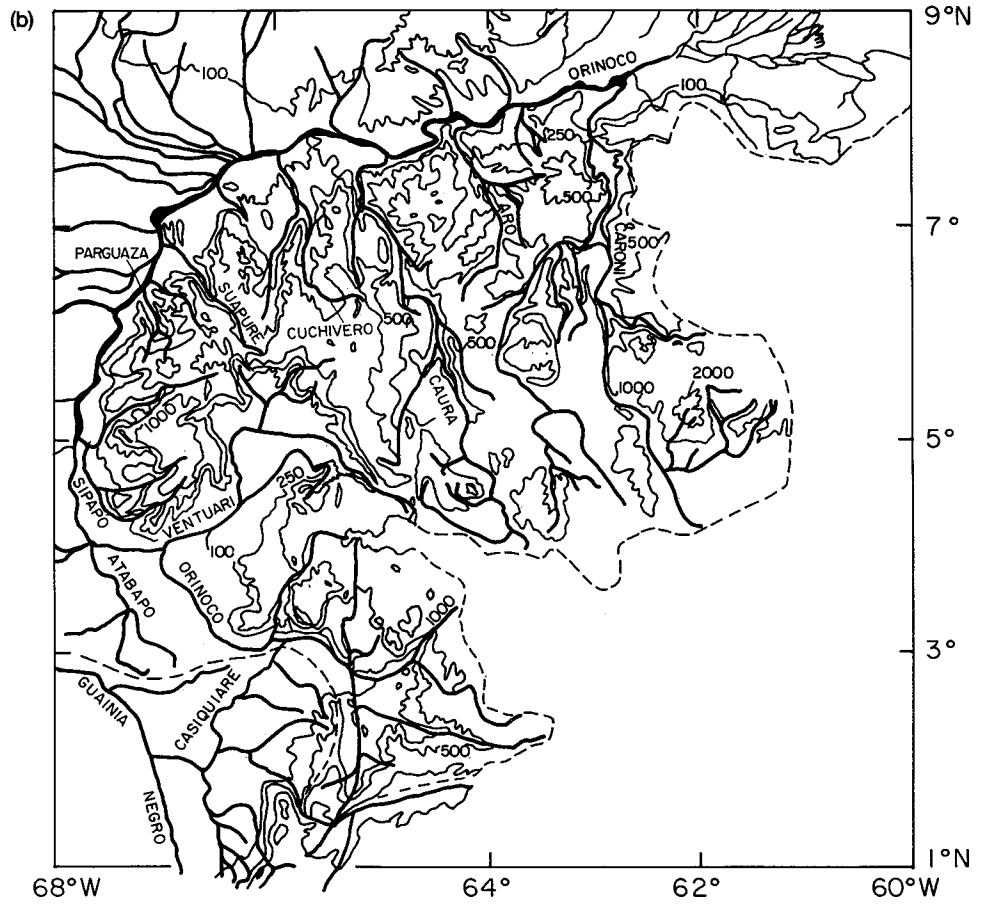

FIG. 1. (Continued)

(MARNR) of the Government of Venezuela, between 1982 and 1988. The results from the left bank, Andean tributaries will be presented elsewhere.

The several countries in the region (Brazil, Colombia, French Guiana, Guyana, Surinam, Venezuela) have their own conventions for the naming of the Shield. This paper will adhere to the term "Guayana" since this is the Venezuelan usage.

2. THE GUAYANA SHIELD

The Guayana Shield (Fig. 1a,b) is the northern extension of the Amazonian Platform and is separated from the Central Brazilian Shield to the south by the Amazon Trough (Gibbs and Barron, 1983, 1993; Sidder and Mendoza, 1991). The boundary of its continuous exposures to the north and northwest is coincident with the main channel of the Orinoco River. Beyond this, it forms the basement of the major, oil-producing sedimentary basins of the Andean Foredeep, the Llanos. In the southwest the Shield is very low-lying and outcrops throughout the headwater drainages of the Orinoco and into those of the Rio Negro in southeastern Colombia and northern Brazil.

The existing information on the geology of the Guayana Shield is discussed in detail in recent monographs by Gibbs and Barron (1993) and USGS (1993). The only evidence for an Archean age for rocks of the Shield comes from model Pb-Pb dates on zircons from gneisses of the Imataca Complex (Montgomery and Hurley, 1978; Montgomery, 1979). This elongate block extends along the right bank of the lower Orinoco and is in fault contact with the other, younger Precambrian rocks of the Shield (Kalliokoski, 1965). The protolith is composed of predominantly acidic, calc-alkaline igneous rocks with minor intermediate rocks, metasediments, Fe formation, and dolomitic marbles (Dougan, 1977). While these appear to have formed in excess of 3.4 b.y. ago, the metamorphic peak (granulites, amphibolite facies gneiss) occurred during the regional Trans-Amazonian event at 2.0 b.y. (Montgomery and Hurley, 1978; Onstott et al., 1989).

The eastern part of the Shield is composed of greenstone belts typical of their Archean counterparts on other cratons. The chemistries of the intrusive and volcanic rocks, the common occurrence of pillow lavas and the composition and structures of the sediment fill indicate that these belts are completely of marine origin with no evidence of a continental source for any of the metasediments (Gibbs and Barron, 1983, 1993; Gibbs et al., 1986). However, they have much younger zircon protolith ages (2.25 b.y.) than those on other Shields (Gibbs and Olszewski, 1982; Gruau et al., 1985). They also have been affected by the Trans-Amazonian event. In the Orinoco drainage, greenstone belts are present in the watershed of the Aro and in the headwaters of the Caura (Fig. 1a).

The igneous and metamorphic rocks of the central Shield give Trans-Amazonian ages with no evidence of an older protolith (Priem et al., 1971). The granitoid intrusives are very extensive, complex, and little studied, due to deep weathering profiles and dense forest cover. In general, they appear to be of calk-alkaline affinity although some small mafic intrusions have also been reported. After the Trans-Amazonian event, the Shield experienced a long period of erosion followed by the deposition of mature sandstones, conglomerates, and shales (Gibbs and Barron, 1993; Sidder and Mendoza, 1991).

In the Middle Proterozoic the Uatuma Supergroup volcanics and associated intrusives were emplaced in the central part of the Shield. These igneous rocks show both calc-alkaline and alkaline trends and give ages of between 1.9 and 1.7 b.y. Most are undeformed and only slightly metamorphosed.

Subsequent to the Uatuma igneous event a major platform cover, the Roraima Group, was deposited over the entire Shield west of the greenstone belts (Rogers et al., 1984). The Roraima reaches a maximum thickness of about 2.5 km in the southeastern part of the Orinoco drainage (Reid and Bisque, 1975; Briceño and Schubert, 1990). It is generally exposed as gently dipping mesas or "tepuy" often with relative elevations of over a kilometer (Chalcraft and Pye, 1984). Extensive mafic intrusives occur in the lower part of the Roraima. The main sedimentary units were deposited in fluvio-deltaic and lacustrine environments and are composed of orthoquartzites, arkoses, and conglomerates with minor shales and jasperoid tuffs. The latter are thought to be associated with the intrusive activity and give ages of 1.65 to 1.73 b.y. (Priem et al., 1973; Gaudette and Olszewski, 1985; Snelling and McConnell, 1969). The conglomerates are diamontiferous and Au-bearing (Reid and Bisque, 1975; Meyer and McCallum, 1993). The source of the diamonds is uncertain. A West African origin has been proposed speculatively by a number of authors (Meyer and McCallum, 1993). However, diamond-bearing kimberlite pipes are known and exploited (by primitive techniques) in the western Shield in the drainage of the Cuchivero. These appear to have ages similar to or older than the Roraima (Nixon et al., 1992) and may represent a local source. Alluvial workings are becoming increasingly common in the eastern outcrop areas. The Roraima and its mafic members are in continuous outcrop in the upper Caroni basin. The formation also occurs as scattered outliers, usually very large mesas or tepuy, as far west as the Rio Negro.

Between 1.56 and 1.43 b.y. there was widespread intrusion of anorogenic granitoids in the western part of the Shield (Gaudette and Olszewski, 1985). This is the youngest such episode on the craton. The largest of these intrusions is the Parguaza batholith which is located inside the major eastwards bend in the course of the Orinoco (Fig. 1a). It has been thoroughly dated at 1.55 b.y. (Gaudette et al., 1978). Many of the granites formed in this episode have rapakivi textures. During the period 1.3 to 1.0 b.y., the western Shield in Colombia was affected by extensive high-grade metamorphism, the Nikerie event (Priem et al., 1982; Gaudette and Olszewski, 1985). There is some uncertainty as to whether this represents the addition of new crust or the thermal resetting of preexisting Trans-Amazonian basement. The subsequent geologic history of the Shield within the Orinoco basin has been restricted to the extrusion of isolated alkali volcanics and to regional uplift in the Mesozoic and Tertiary, especially in the east (Fig. 1b), associated with the opening of the Atlantic (Sidder and Mendoza, 1991).

The geology of that portion of the Guayana Shield drained by the Orinoco is remarkable for the complete absence of limestones or evaporites of marine or lacustrine origin. With the exception of the Roraima Formation, the weathering substrate is almost entirely composed of igneous and metamorphic rocks. Thus, over large areas, the weathering is "first cycle," involving only Precambrian basement rocks and making it possible to examine crustal weathering processes in detail (Lopez and Bisque, 1975; Schorin and Puchelt, 1987). In this regard, the region is rather unique, since in most other large drainages, extensive outcrops of rapidly weathering Phanerozoic biogenic and chemical sediments largely obscure the primary signal from the crust (Hu et al., 1982; Stallard and Edmond, 1983; Reeder et al., 1972).

The Orinoco rises in the Sierra Parima in the central part of the Shield at elevations greater than 1,000 m. It is 2,150 km in length and drains an area of 850,000 km^2, about one half of which is exposed Shield. The annual average discharge of $1,200 \times 10^9$ m^3/y makes the Orinoco the third largest river in the world after the Amazon and Congo, supplying ~3.6% of the global runoff (Meade, 1994). The drainage of the Orinoco is separated from that of the Rio Negro/Amazon to the southwest by ill-defined and swampy divides. Its headwaters are undergoing active capture by the Negro via the Casiquiare (Fig. 2), which currently diverts ~20% of the headwater discharge into the Amazon system, mainly at flood stage. The river flows west and north, with the Ventuari and Sipapo being the major right bank tributaries. At 4°N the river course begins a broad eastwards bend around the Parguaza batholith. The topography of the bordering Shield becomes more mountainous with elevations exceeding 1,000 m. Andean detrital sediments, transported dominantly by the three major left bank tributaries, the Guaviare, Meta, and Apure, onlap the Shield and, in the absence of a significant detrital flux from the right bank streams, constrain the Orinoco channel such that it defines the contact. Thus, in striking contrast to the Amazon, the river is a bedrock stream over much of its course with several extensive rapids. Meanders are developed only along one section of the lower river a few hundred kilometers long.

The climate of the entire basin is tropical save in the higher elevations of the Andes and the southeastern Shield. In the lower courses of the river and on the high Shield the rainfall distribution is strongly seasonal reflecting the northwards excursion of the Equatorial Trough and its interaction with the Northern Trades. The rainy season extends from April through October. The highlands receive about 2 m of rain per year. On the lowland Shield precipitation is high throughout the year with a total in excess of 3 m. Over the rest of the Basin the dry season (November to March) is extremely pronounced. In the southwest the peak discharge occurs in June and July. Farther north, in the Andean streams and the lower Orinoco, the maximum flood stage is in mid to late August (Fig. 3). The stage height of the lower Orinoco oscillates over about 15 m annually and the associated discharge varies by up to a factor of 20–30 (Nordin and Perez-Hernandez, 1989; Meade, 1993). Major Shield tributaries essentially dry up seasonally being maintained solely by weak groundwater flow.

The left bank of the river, the Llanos, is a "trade wind desert" which supports only cactus and low scrub. The Trades remobilise sand from the fluvial bars exposed at low stage and transport it upriver feeding a 20,000 km^2 tract of active dunes west of Cabruta, downstream from the Apure confluence (Fig. 2; Nordin and Perez-Hernandez, 1989; McKee, 1989). At the time of the last glacial maximum most of the Llanos was a sand desert with numerous fields of large dunes (Clapperton, 1993a,b). These are clearly visible from the air and in satellite pictures.

Previous published work on the geochemistry of the Orinoco is limited to the investigations of Lewis and his coworkers on the lower river (Lewis and Weibezahn, 1981; Lewis et al., 1986; 1987), by Weibezahn (1985, 1990) on the middle and upper Orinoco, and by Vegas-Vilarrubia et al. (1988) on the black water streams. Lewis et al. (1986, 1987) emphasized the extremely dilute nature of the two Shield tributaries they studied, the Caroni and the Caura. A two year time-series for the Caura allowed Lewis et al. (1987) to arrive at quite accurate estimates of the denudation rate of that basin. There appear to be no published chemical data for other large rivers of the Shield.

3. SAMPLING AND ANALYSES

Sampling was timed, where possible, to coincide with the extrema in the discharge and with the midpoints of rising and falling stage (Fig. 3). The river is navigable by shallow-draught barge to the rapids at Puerto Ayacucho above the confluence with the Meta, a major left bank Andean tributary. Below Ayacucho samples were collected from the Shield rivers close to their confluences using small boats deployed from the barge DUIDA. The headwaters of these streams and the Basin above Ayacucho were reached by road, light plane, or helicopter. There samples were collected from mid-channel using small boats and canoes or, where these were not available, from the bank on the outside of bends where the flow was most vigorous. Some samples from particularly inaccessible areas, e.g., the left bank tributaries to the Casiquiare, were collected by MARNR personnel during hydrologic investigations. Because of logistical difficulties in the rainy season, access to the headwaters and to the basin above Puerto Ayacucho was restricted to the dry season. In addition, access to many of the downstream tributaries was impeded because of navigation problems in the deeply inundated terrain. Thus, the flood crest is markedly undersampled (Fig. 3). Measurements of discharge and suspended load transport by this project could only be made on the tributaries below Ayacucho. However, MARNR operates an extensive network of calibrated gauging stations throughout the headwaters of the Orinoco as does the hydropower company EDELCA on the Caroni.

All samples were collected in 500 mL linear polyethylene bottles that had been leached with deionized, distilled water for at least 24 h at 60°C. This cleaning procedure was necessary because of the anticipated extremely dilute nature of many of the streams to be sam-

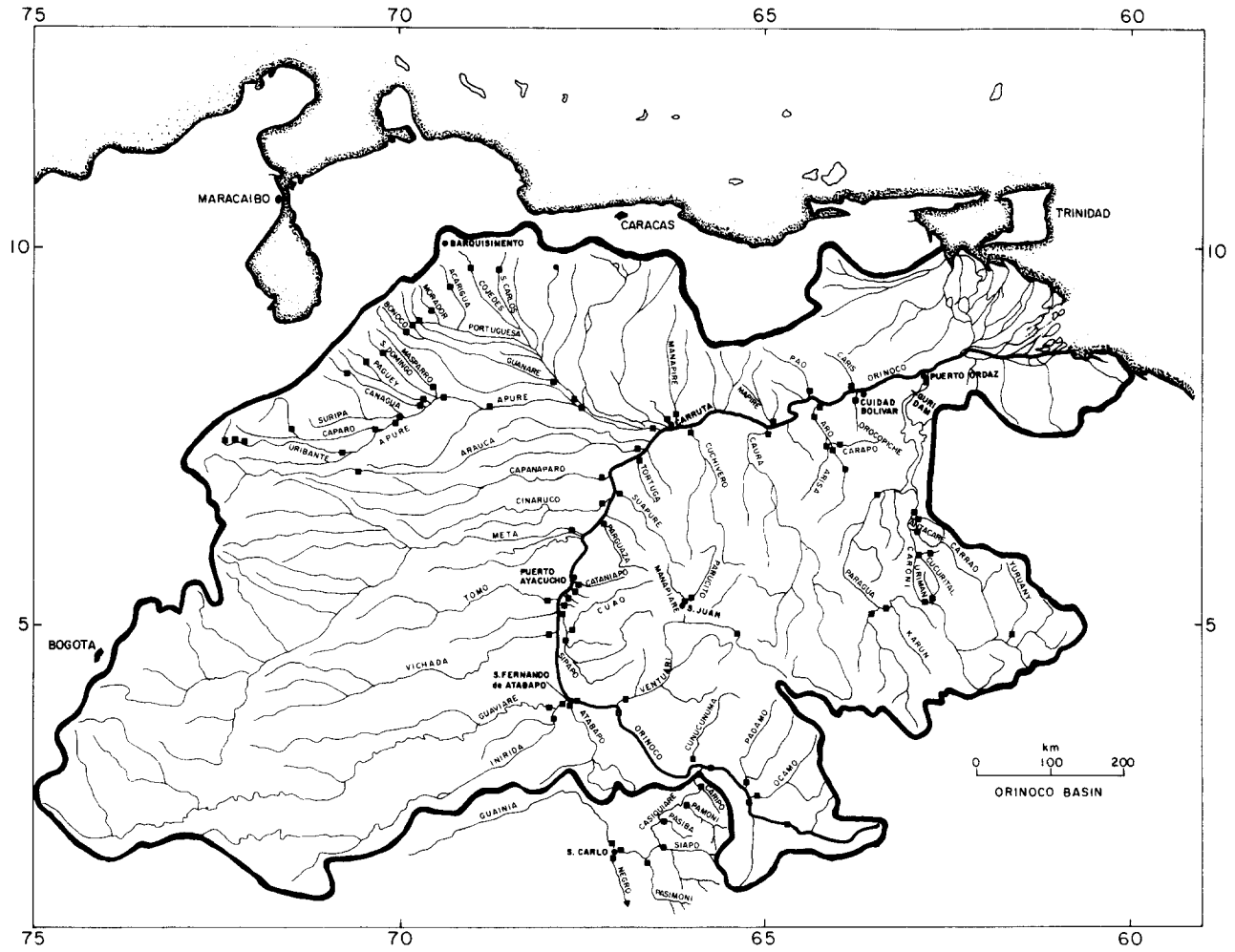

FIG. 2. Location map of sample sites in the Orinoco basin. The data from the left bank Andean tributaries will be presented elsewhere.

pled. Bottles were supplied to MARNR for their collection programs. Where the equipment was available and working, pH was measured while the samples were being collected. Measurements made on stored filtered samples were found to be spurious. Where possible, samples were filtered within a few hours of collection. For the chemical components under discussion here, distilled water washed Millipore filters of 0.45 μm nominal pore size were used. Samples collected from remote areas sometimes had to be stored for several days before filtration, either on the DUEDA or in the MIT laboratory. The samples collected by MARNR were several weeks old when filtered.

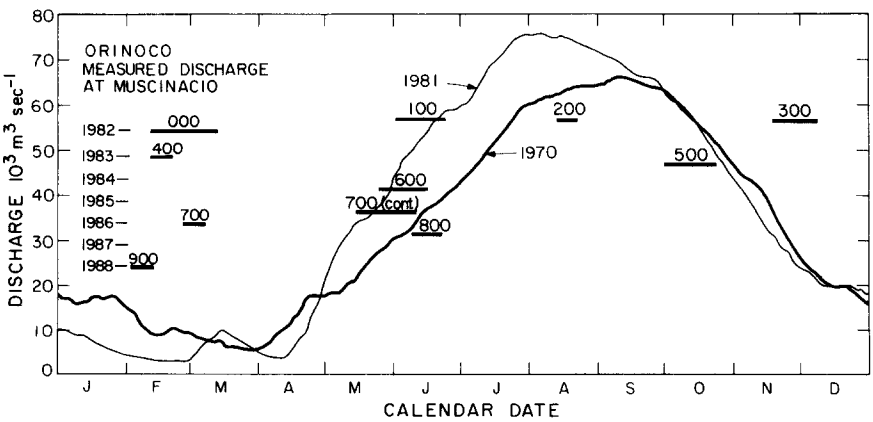

FIG. 3. Annual discharge of the Orinoco at Musinacio above C. Bolivar on the lower river. Two representative hydrographs are shown. The sampling periods are indicated by the horizontal bars with the series number as used in the data tables.

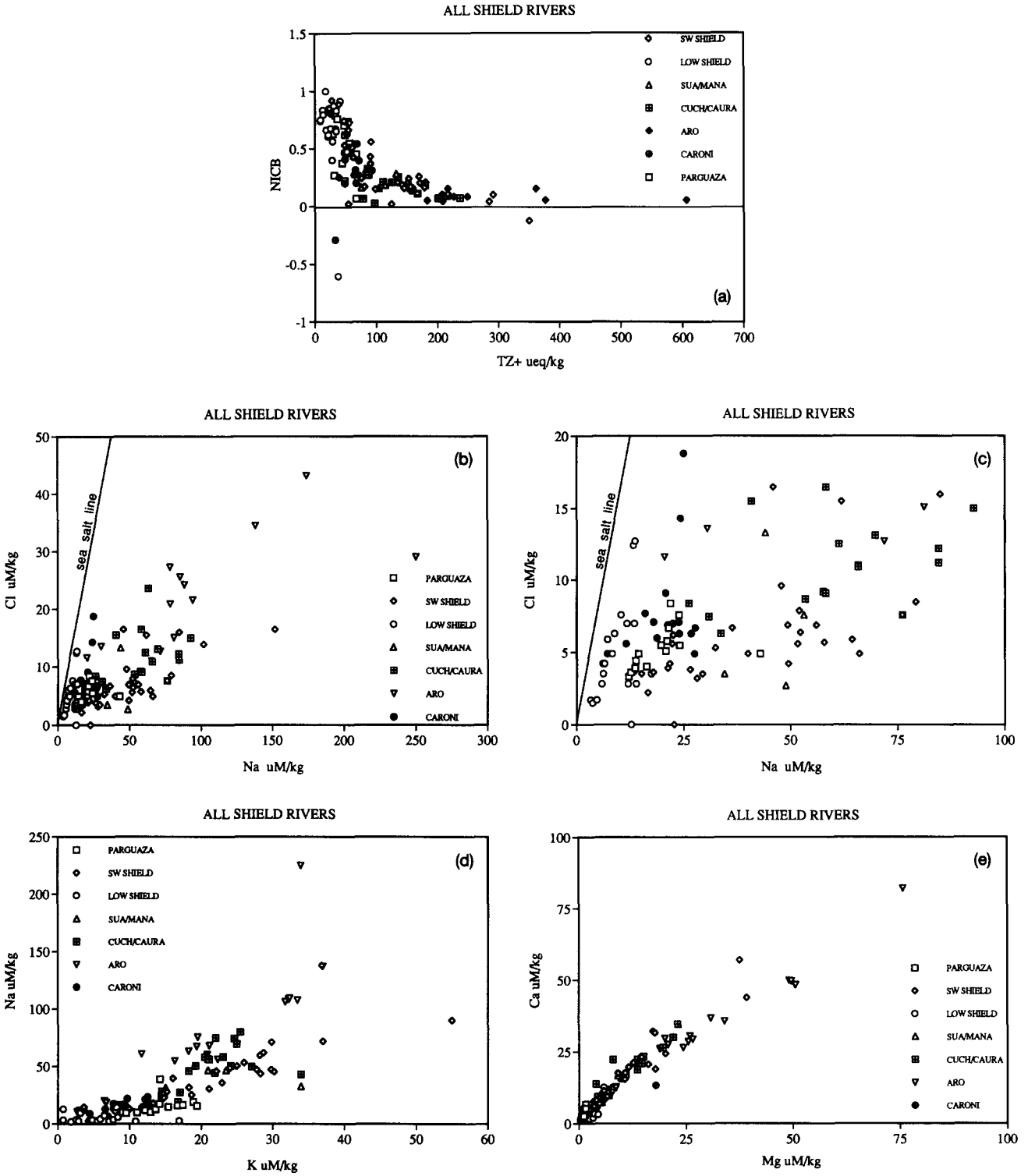

FIG. 4. (a) The Normalised Inorganic Charge Balance (NICB), defined as $([TZ^+ - TZ^-]/TZ^+)$, versus total cationic charge (TZ^+). Protons are not included in TZ^+ since data are not always available. For samples with negative "alkalinities" the value is set to zero in the calculation of NICB. The three points that indicate strongly negative NICB appear to have unexplained high alkalinity. (b–e) Property-property diagrams for the rivers draining the Shield. In the Na-Cl plots the sea-salt ratio is indicated by the line. *In all subsequent plots, the data are corrected for the sea salt component as described in the text.*

TABLE 1 * CHEMICAL DATA FOR STREAMS DRAINING THE PARGUAZA BATHOLITH

River name	sample number	date d/m/yr	Na uM/kg	K uM/kg	Mg uM/kg	Ca uM/kg	Cl uM/kg	SO_4 uM/kg	alkalinity ueq/kg	Si uM/kg	pH	$^{87}Sr/^{86}Sr$ **	Sr nM/kg	Rb nM/kg	Cs pM/kg
Parguaza	011	03/03/82	24.1	19.0	1.7	4.9	5.5	1.0	18	127	-	-	-	-	-
	157	18/06/82	16.3	13.7	2.0	5.4	4.0	1.0	22	81	5.6	0.8189	20.0	41	244
	309	22/11/82	19.7	15.5	1.5	4.5	5.5	0.8	7	96	5.9	0.8535	16.7	45	433
	461	07/03/83	21.5	19.5	2.1	5.2	6.7	1.0	21	111	6.2	0.8434	22.4	61	527
	531	13/10/84	23.9	14.3	1.5	3.6	7.6	0.0	30	90	5.8	0.8429	16.1	41	306
Cataniapo	305	18/11/82	21.1	16.8	1.5	4.0	5.8	0.8	11	104	4.8	0.9058	14.1	52	590
	549	17/10/84	43.0	14.3	1.5	3.7	4.9	4.1	50	88	5.9	-	-	-	-
Paria Grande	352	18/11/82	20.9	17.5	1.9	5.6	5.1	0.4	8	94	4.3	0.8620	19.5	54	630
Samariapo	353	"	13.8	11.1	1.2	2.9	4.4	0.3	2	72	4.9	0.9117	10.8	36	480
Sipapo @ mouth	354	"	12.6	9.6	1.0	2.6	3.6	0.7	-10	70	3.8	0.9098	8.4	34	409
	580	19/10/84	13.6	9.1	1.0	2.3	3.9	0.0	7	57	-	-	-	-	-
	601	24/05/85	12.1	12.2	1.2	2.6		0.0	20	64	5.5	-	-	-	-
Sipapo ab Cuao	480	06/03/83	14.5	13.0	1.4	3.0	4.9	1.9	-10	68	4.8	0.9217	9.9	45	496
Cuao ab Sipapo	481	"	21.8	27.0	2.4	6.9	8.4	1.3	26	98	5.0	0.9024	24.1	90	1094

* The tabulated concentration measurements are uncorrected for the effects of the aeolian deposition of sea salts. The data plotted in the Figures are so corrected using the assumption that all the chloride in the streams is of marine origin and that the other ions are delivered in their sea salt ratios to chloride (see discussion in text).
Units: uM = 10^{-6} moles; nM = 10^{-9} moles; pM = 10^{-12} moles; ueq = 10^{-6} equivalents.

** The tabulated $^{87}Sr/^{86}Sr$ data are corrected for the effects of the input of sea salt strontium.

Storage tests on unfiltered vs. filtered Orinoco samples and on similar ones collected in the Amazon Basin (Stallard, 1980) showed no significant chemical effects over a period of more than a month; measurements were reproducible to within analytical uncertainty. In order to extend coverage of the Shield into northern Brazil, samples from a previous study of the Amazon Basin are included (Stallard and Edmond, 1983). These characterize the Rio Branco, which drains the region south of the headwaters of the Orinoco, and the Rio Negro above its confluence with the Branco, which includes a major part of the drainage of the Lowland Shield.

The major cations, Na, K, Mg, and Ca, were analysed by flame atomic absorption. Sulfate and Cl were determined by ion chromatography, alkalinity (or acidity) by acid titration with end-point determination by Gran plot (Edmond, 1970), and Si by spectrophotometric measurement of the Mo blue complex. Analytical errors were determined both by repeat analyses and by measurements on duplicate samples. Over the concentration ranges encountered the AA and IC data had 2-sigma errors of better than 2%, alkalinity 0.5%, and Si 1%. Since samples were analyzed in the batches collected on each field expedition several samples from the first expedition were reanalyzed with each succeeding batch as a check on internal analytical consistency and a further check on reproducibility.

The minor cations Rb, Cs, and Sr were analyzed on selected samples by isotope dilution, mass spectrometry (MSID). The isotopic composition of the dissolved strontium was also determined on these samples (Palmer and Edmond, 1989, 1992). Since the temporal variation in the isotopic composition of a particular stream is quite large (e.g., the observed $^{87}Sr/^{86}Sr$ range in the Parguaza is from 0.8189 to 0.8535, depending on season), it was not necessary to achieve "geochronologic" accuracy. In many cases, this was precluded a priori because of very low Sr abundances or, in the case of the most dilute streams, by the magnitude of the sea salt correction; this can affect the third figure in the ratio. Potassium was also measured by MSID on these samples as a check on the flame AA data. Barium was measured by ICP–MS using isotope dilution (Klinkhammer and Chan, 1990).

The isotopes of beryllium, ^{9}Be and cosmogenic ^{10}Be, Bi, Se, Ge, Re, U, and the concentration and isotopic composition of the particulate organic carbon have also been measured on a number of the samples in connection with other projects. These data are presented elsewhere (Measures and Edmond, 1983; Brown et al., 1992; Lee et al., 1986; Yee et al., 1987; Murnane and Stallard, 1990; Colodner et al., 1993; Palmer and Edmond, 1993; Tan and Edmond, 1993). Parallel studies have also been published on the detrital load (Johnsson et al., 1988; Johnsson, 1990; Savage and Potter, 1991) and on sediment transport processes (Stallard, 1987; McKee, 1989; Nordin and Perez-Hernandez, 1989; Meade et al., 1990a; Meade, 1994).

4. DISCUSSION OF THE DATA

In order to gain an overall impression of the geochemistry of the waters draining the Guayana Shield a summary discussion of the complete major ion dataset will first be presented. For detailed examination, the data will then be grouped based on the geology and elevation of the various drainages. Finally, the discharge and sediment transport data will be combined with the water chemistry to yield estimates of the denudation rate of the various sub-basins and of the Shield as a whole.

The rivers draining the Shield are all remarkably dilute (Tables 1–7). The total cationic charge ($TZ^+ = Na^+ + K^+ + 2\{Mg^{2+} + Ca^{2+}\}$; Fig. 4) in the samples analyzed ranges from a high of ~600 μeq/kg (10^{-6} equivalents/kg) to lows of around 40 μeq/kg (~10 μeq/kg if protons are not included). The bulk of the samples have values below 100 μeq/kg. For comparison, the "world average river water" has an estimated TZ^+ of 1,200 μeq/kg (Meybeck, 1979). The analytical data show a substantial charge imbalance, particularly in the more dilute waters, similar to that observed previously in the flood plain rivers of the Amazon (Stallard and Edmond, 1983), in the Caura (Lewis et al., 1987), and in the Congo (Négrel et al., 1993). Usually, these waters have a negative "alkalinity" and a pH sufficiently low that protons are the major cationic species. The most dilute streams have concentrations of inorganic anions (chloride, sulfate, carbonate, bicarbonate) that are essentially zero. The magnitude of the imbalance is best seen in a plot of the Normalized Inorganic Charge Balance ($NICB = \{TZ^+ - TZ^-\}/TZ^+$) against TZ^+ (Fig. 4; Stallard and Edmond, 1983; $TZ^- = Cl^- + HCO_3^- + 2SO_4^{2-}$). The NICB increases with decreasing overall concentrations; values approaching 100% are common at low TZ^+ (<50 μeq/kg) and may be even larger depending on the (unmeasured) concentrations of dissolved Fe and Al. The imbalance requires the presence of anions not analyzed directly and with low association constants. These must be organic. In fact the acid rivers are invariably "black" with high concentrations of dissolved organic carbon. Lewis et al. (1986) reported relatively constant values for DOC of around 5 ppm (~400 μmol C/kg: 10^{-6} mol C/kg) in their study of the Caura. Thus, it can be inferred that organic acids not only control the acidity of these streams but that, given the large charge imbalance, they may also be responsible for a substantial part of the weathering.

It did not prove possible to collect uncontaminated samples of rainwater; hence the correction for the contribution of "cyclic salts" of marine origin to the dissolved load of the

streams cannot be made directly. The Cl concentrations range up to 45 μM (10^{-6} mol/kg); however, the majority of the values are below 10 μM (Fig. 4). Most of the higher values are from the drainages of the Aro and Cuchivero. On an Na-Cl diagram the low concentration boundary is sharp, parallels the sea-salt line, and is displaced from it slightly (<5 μM) to higher Na values (Fig. 4). The Na:Cl ratio in the high-Cl samples is approximately 5, much too low to be derived from the weathering of Shield rocks. The discharges of both the Aro and the Cuchivero have relatively restricted contributions from highland areas (>1,000 m elevation) as compared to the rest of the Shield rivers (Fig. 1b). This is especially true of the Aro. The higher Cl in these rivers probably reflects the greater relative contribution of seasalt aerosol from the lower troposphere to the local rainfall in these low-lying basins. Since the concentrations of Cl in the Shield rivers are within the range observed for streams draining the Amazon floodplain (Stallard and Edmond, 1981, 1983) it seems reasonable to assume that all of it is of marine origin. Lewis et al. (1987) reached the same conclusion in their study of the Caura where they were able to collect a time series of total fallout (wet plus dry deposition). Their fluvial values ranged from 5 to 26 μM and represented a flux equivalent to the measured atmospheric inputs. The values observed here in the rivers draining the lowland Shield (1.5–12.7 μM, average 4.2 μM) are consistent with those reported in rain samples collected at San Carlos de Rio Negro, at the confluence of the Guainia-Negro and the Casiquiare (0.0–11.6 μM, volume-weighted mean 2.5 μM; Galloway et al., 1982). They also agree well with the values reported for rain at several locations in the central Amazon basin (Andreae et al., 1990). The San Carlos data give a Na:Cl ratio of 0.72 in reasonable agreement with value of 0.86 for sea salt. However, the ratios for K, Ca, and especially sulfate are much higher. Similar results were reported by Stallard and Edmond (1981) for Amazonian rain, Lewis et al. (1987) for the Caura, and Négrel et al. (1993) for the Congo; it can be concluded that these excesses over what would be expected for a pristine marine aerosol must originate by biogenic and other processes occurring within the basin. Hence, strictly, they are part of the weathering flux. Assuming that all the Cl is cyclic and that the other cations are added in their sea-salt ratios, then the resulting correction to the data is important only for Na, with values in the most dilute streams of the Lowland Shield of around 40%, and Mg where the largest corrections are between 15 and 25%. Since most of the primary Cl in the Shield rivers must be derived from fluid inclusions of NaCl brines in the igneous and metamorphic rocks, the exact validity of the Cl correction used here does not significantly affect the discussion of mineral weathering reactions and processes. The rain-derived K and Ca are an insignificant component of the totals observed in the streams. The fluvial sulfate values are usually substantially lower than those reported in the rain. This was also observed in the Amazon and must reflect accumulation of S in the biomass and its recycling through the local atmosphere following decomposition (Montes et al., 1985).

On a K-Na diagram (Fig. 4) most of the data plot in a range of K:Na ratios of between 0.8 and 0.3 with the upper bound defined by the Lowland Shield and the Parguazan drainages. The Carapo and the Oropiche, which drain the Imataca Complex, are much more sodic with ratios of 0.2 and below. On a Mg-Ca diagram (Fig. 4), the data define a linear array corresponding to a Mg:Ca ratio of about 0.7 overall. The Parguazan drainage is more calcic with a ratio of 0.25 and the Aro, which includes greenstone belts in its drainage, is more magnesian (Mg:Ca ~ 1). The Lowland Shield rivers are also very magnesian (Mg:Ca ~ 2). The cation ratio plot {K/(Na + K) vs Mg/(Mg + Ca)} displays two trends (Fig. 5). One is the conventional differentiation trend for igneous rocks going from a high value for the alkali ratio and a low one for the alkaline earths (Parguaza granite) to a low alkali and high alkaline earth ratio (Aro amphibolites). A distinctly different, positive trend is defined by the rivers of the Lowland Shield. The fractionation of K and Mg from Na and Ca is a general characteristic of partial weathering. The positive slope is indicative, therefore, of continued reaction of transported fluvial detritus, presumably of Andean origin. A much less well-defined trend of the same type is developed by streams draining the flood plain of the Amazon (Stallard and Edmond, 1983). The relationship between Si, TZ^+, and [Na + K] is also shown in Fig. 5. The weathering of average Shield rocks to kaolinite and gibbsite gives ratios Si:[Na + K] of 1.7 and 3.5, respectively, assuming no quartz dissolution (Stallard and Edmond, 1983). Most of the data fall within these two limits indicating complete removal of the soluble cations.

The ternary anion diagram [Si, Alkalinity, ($Cl^- + 2SO_4^{2-}$)] was used by Stallard and Edmond (1983) as a diagnostic tool in the characterization of weathering regimes (see also Hu et al., 1982; Berner and Berner, 1987). It is not particularly informative here, since in the absence of an inorganic charge balance, the alkalinity has no fundamental significance. All the data fall along the Si-Alkalinity join strongly displaced to high Si. On a ternary cation diagram, [$2Mg^{2+}$, $2Ca^{2+}$, ($Na^+ + K^+$)], the data fall on a linear trend extending from close to the (Na + K) apex, and displaced from it towards Ca, out into the central part of the triangle (Fig. 6). Points computed from published estimates of the chemical compositions of average igneous rock types (Wedepohl, 1969) fall within the data envelope or along its extension. Thus, to a first approximation, weathering processes on the Shield go to completion with little resolvable retention of the major cations in secondary phases. Lewis et al. (1987) reached the same conclusion for the Caura based on calculations of the weathering mass balance. Both these approaches depend on data for "average" rock units since little information is available on the rocks of the Guayana Shield itself. A much more direct estimate of weathering intensities can be gained from examination of the trace cations Rb, Cs, and Ba and of Sr and its isotopic systematics.

The geochemical properties of the alkalis and alkaline earths vary in a systematic way as one moves down the Periodic Table with Cs and Ba having the highest retention in structural and surficial ion-exchange sites in secondary minerals. The relationship between Rb and Sr and $^{87}Sr/^{86}Sr$ in solution can also be used, in comparison with geochronometric values for whole-rocks reported from the various basins, to identify environments where fractionation, i.e., incomplete weathering, occurs. In igneous processes, Sr is partitioned into more readily weathered minerals such as Ca and Na-feldspars while the more resistant K-feldspars and micas

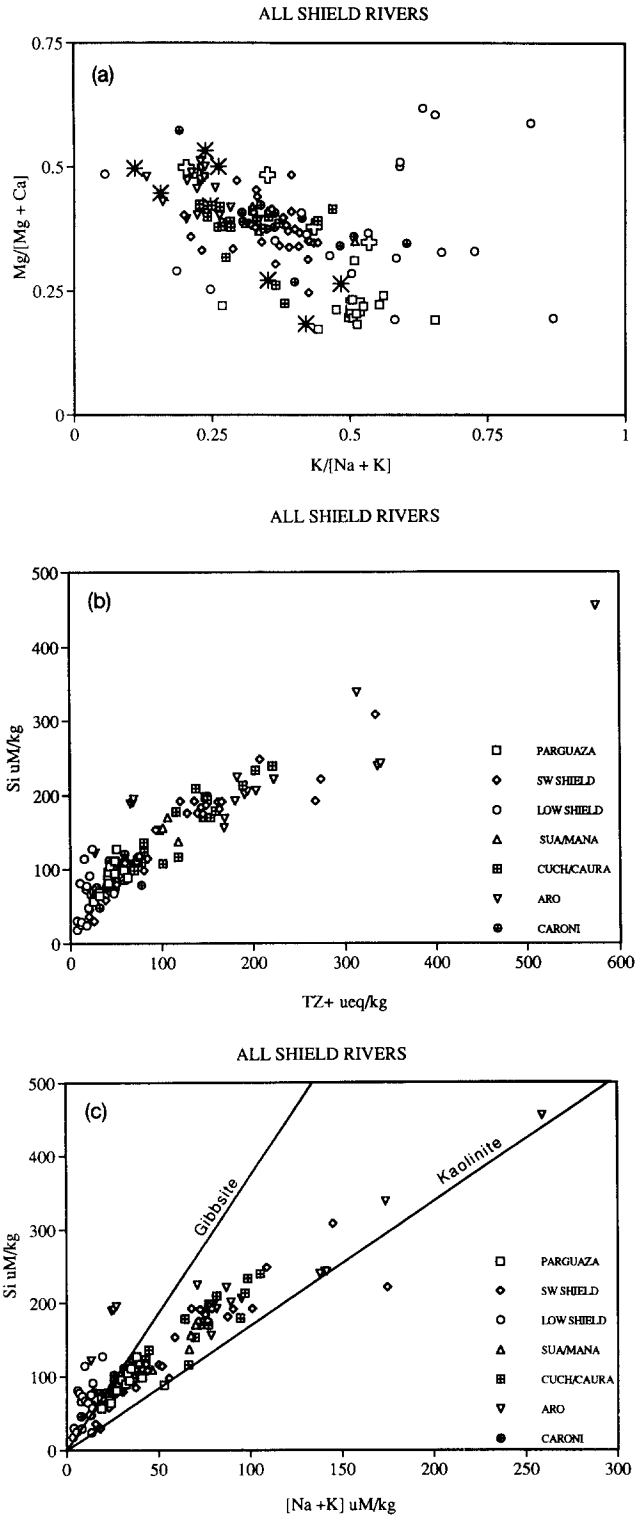

FIG. 5. (a) The relationship between the ratios Mg/(Mg + Ca) and K/(Na + K). The bulk of the data parallel the trend for "average igneous rocks" (open crosses) and the data of Dougan (1977) for the average compositions of the various rock types of the Imataca Complex (stars) and extend to the average composition of the Parguaza Batholith (large square). The points lying off the trend, especially to high alkaline earth ratios indicate the continued weathering of immature, partially weathered detritus transported to the flood plain from the Andes. (b) Si vs. TZ^+ (c) Si vs. [Na + K]. The lines indicate the ratios expected from the weathering of average basement rocks to gibbsite and to kaolinite (assuming no dissolution of quartz).

preferentially take up Rb. Thus, given the great age of the rock-types of the Shield, differences in the initial Rb/Sr ratios between the igneous minerals lead to large differences in their contemporary $^{87}Sr/^{86}Sr$ ratios. As an example Gaudette et al. (1978) reported data from the 1.55 b.y. Parguazan granite for ^{86}Sr, ^{87}Rb, and $^{87}Sr/^{86}Sr$; in the whole-rock the values were 17.5 and 52.6 ppm and 0.7645, respectively as compared to 14.1, 126, and 0.8804 in a K-feldspar mineral separate. Departures of the fluvial systematics from the geochronometric relationships are, therefore, a sensitive indicator of differential weathering and, in combination with the Cs and Ba data, of secondary reactions. The data for the trace cations will be discussed in the following sections.

5. REGIONAL DISCUSSION

The Shield can be divided into various subregions based on geology and topography (Fig. 1a,b). The lithologically homogeneous Parguazan batholith will be discussed first, then the surrounding Trans-Amazonian basement of the southwestern Shield which hosts the headwaters of the Orinoco and the Ventuari, the left bank affluents of the Casiquiare and the southwards flowing Branco, a tributary of the Negro-Amazon system. The data from the very dilute streams of the lowland Shield will then be presented. The Suapure and Manapiare flow north and south (the latter to the Ventuari) along the eastern boundary of the Parguazan granite and so will be discussed together. Moving east, the Cuchivero/Caura basins will be combined, since they are adjacent and geologically similar. Also included will be the Tortuga and the Parucito, a right bank tributary of the Ventuari. Then, the Aro drainage will be examined followed, finally, by the Caroni.

5.1. The Parguaza Batholith

The vast terrain of the Parguazan rapakivi granite batholith, one of the largest of its kind in the world, is drained by two large rivers, the Parguaza and the Sipapo-Cuao (Figs. 1, 2). Numerous smaller streams also drain this massif (Cataniapo, Paria Grande, Samariapo). A major outlier of the Roraima quartzite lies within the drainage of the Sipapo and its tributary, the Cuao. The other streams drain only the granite.

All the streams are quite dilute ($TZ^+ = 20$–70 μeq/kg) with silica values generally below 100 μM, the approximate value for quartz saturation (Table 1). The smaller ones are acid (pH < 5). On property-property diagrams (Fig. 7), the data fall in restricted ranges clustered around the average rock composition reported by Gaudette et al. (1978). Consistent with the highly fractionated nature of the granite, the rivers have the highest K:Na and Ca:Mg ratios of any on the Shield (~1 and 4, respectively). The concentrations of the major alkalis (Na + K) correlate strongly with that of Si; the trend extrapolates to the origin. The Si:(Na + K) ratio is about 3.3 consistent with weathering to gibbsite. Since the trend passes through the origin, there is no resolvable dissolution of quartz or of residual kaolinite. On the alkali-alkaline earth and ternary cation diagrams the data form a cluster around the reported average rock composition.

The rivers draining the Parguaza massif are strongly enriched in the heavy alkalis (Fig. 7). The Cs concentrations

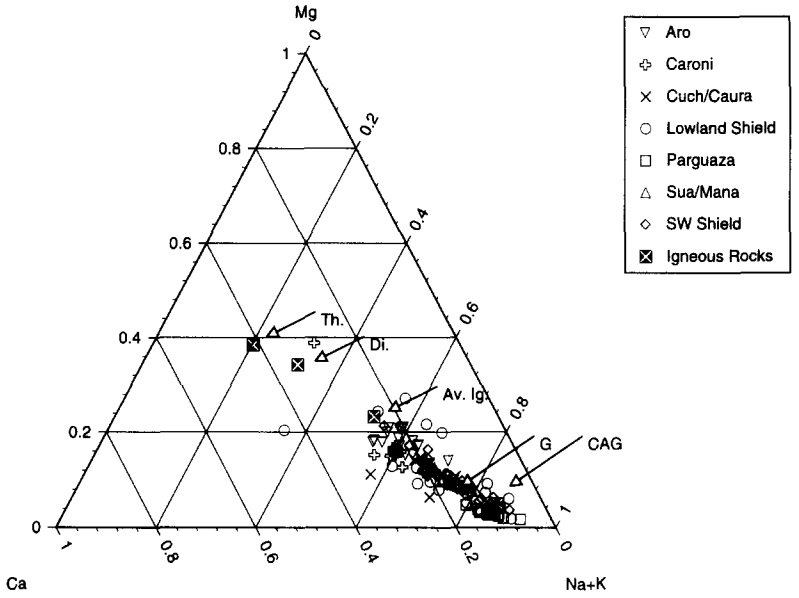

FIG. 6. The ternary diagram for the major cations. The equivalent average compositions of the major igneous rock types are also plotted: CAG = Calc-Alkaline Granite; G = Granite; Av. Ig. = Average Igneous Rock; Di. = Diorite; Th. = Tholeiite.

range to >1 nM (10^{-9} mol/kg), the highest observed on the Shield and, concomitantly, the values for the Na/Rb and Na/Cs ratios are the lowest. These high Rb and Cs levels are strongly correlated (Cs:Rb ~ 0.01) and are presumably the result of the partitioning of these incompatible elements into this anorogenic granite during anatexis (there are no reported Cs values for the batholith itself). In addition, there is a positive relationship between Cs/K and $^{87}Sr/^{86}Sr$ as would be expected since high Cs/K should follow high Rb/Sr in the whole-rock. There is a good linear correlation between Ba and K with the ratio K:Ba ~ 250.

Gaudette et al. (1978) report whole-rock Rb/Sr dates for the batholith of 1.55 b.y. with an initial $^{87}Sr/^{86}Sr$ ratio of 0.7004. They considered their two most radiogenic samples as defining a secondary isochron (1.26 b.y., initial ratio 0.726) correlated with the Nikerie metamorphic event recognized as partially resetting the Rb/Sr systematics in this region. The two isochrons that they obtained are plotted in Fig. 8 together with the river measurements. These all fall on, or very close to, the whole-rock isochrons. The data fall in two elongate clusters. The Parguaza river itself, draining the northeast quadrant of the batholith, is less enriched in the heavy alkalis and has less radiogenic Sr (0.8189–0.8535) as compared to the Sipapo-Cuao and the smaller streams in the west and south (0.9024–0.9217). The latter values are among the highest observed fluvial values anywhere and are substantially above any reported for the whole-rocks which were, in fact, collected "in the Suapure River region" (Gaudette et al., 1978), i.e., along the eastern outcrop of the batholith. The Rb-Sr systematics strongly suggest that there is no preferential release of less-radiogenic Sr associated with easily weathered minerals poor in Rb such as Na and Ca feldspars. Thus, as inferred from the major element data and the Cs and Ba systematics, weathering is complete. Despite the presence of a major outlier of the Rorima formation in the Sipapo-Cuao drainage there is no indication of its providing a significant contribution to the dissolved load. In fact the highest Cs, Ba, and K concentrations and the most radiogenic Sr values on the Shield come from this sub-basin. The K:Na ratio is as high as 1.24 in the single sample from the Cuao.

Samples were collected at the mouth of the Parguaza in June and November of 1982, March 1983, and October 1984. The $^{87}Sr/^{86}Sr$ ratios range from 0.8535 to 0.8189. All four samples fall on the whole-rock isochron and on the Cs/K vs. $^{87}Sr/^{86}Sr$ relationship defined by all the stream samples draining the batholith. Hence, the data reflect compositional differences in the sources of the dissolved material within the terrain of the batholith rather than seasonal changes in the intensity of weathering.

5.2. The Southwestern Shield

The headwaters of the Orinoco above its confluence with the Ventuari, the Ventuari itself above the Manapiare, the left bank tributaries of the Casiquiare and the southwards flowing Rio Branco (a tributary of the Negro-Amazon in Brazil) drain a large area of "undifferentiated Proterozoic rocks" (Sidder and Mendoza, 1991), the Trans-Amazonian Basement of the southwestern Shield (Fig. 1). The upper reaches of all these streams are hilly with elevations in excess of 500 meters. The Orinoco-Amazon watershed line, defining the border with Brazil, is commonly at over 1,000 meters. In general, the river courses descend rapidly to elevations less than 100 meters such that most of the basin areas are flat-lying, gently undulating, and heavily forested. Much of the topography in the interior of the basins is formed by outliers of the Roraima quartzite which, as in the case of Cerro Duida at the confluence of the Cunucunuma and the Orinoco, can achieve local elevations in excess of 2,000 meters. What little that has been reported about the regional geology suggests that a wide range

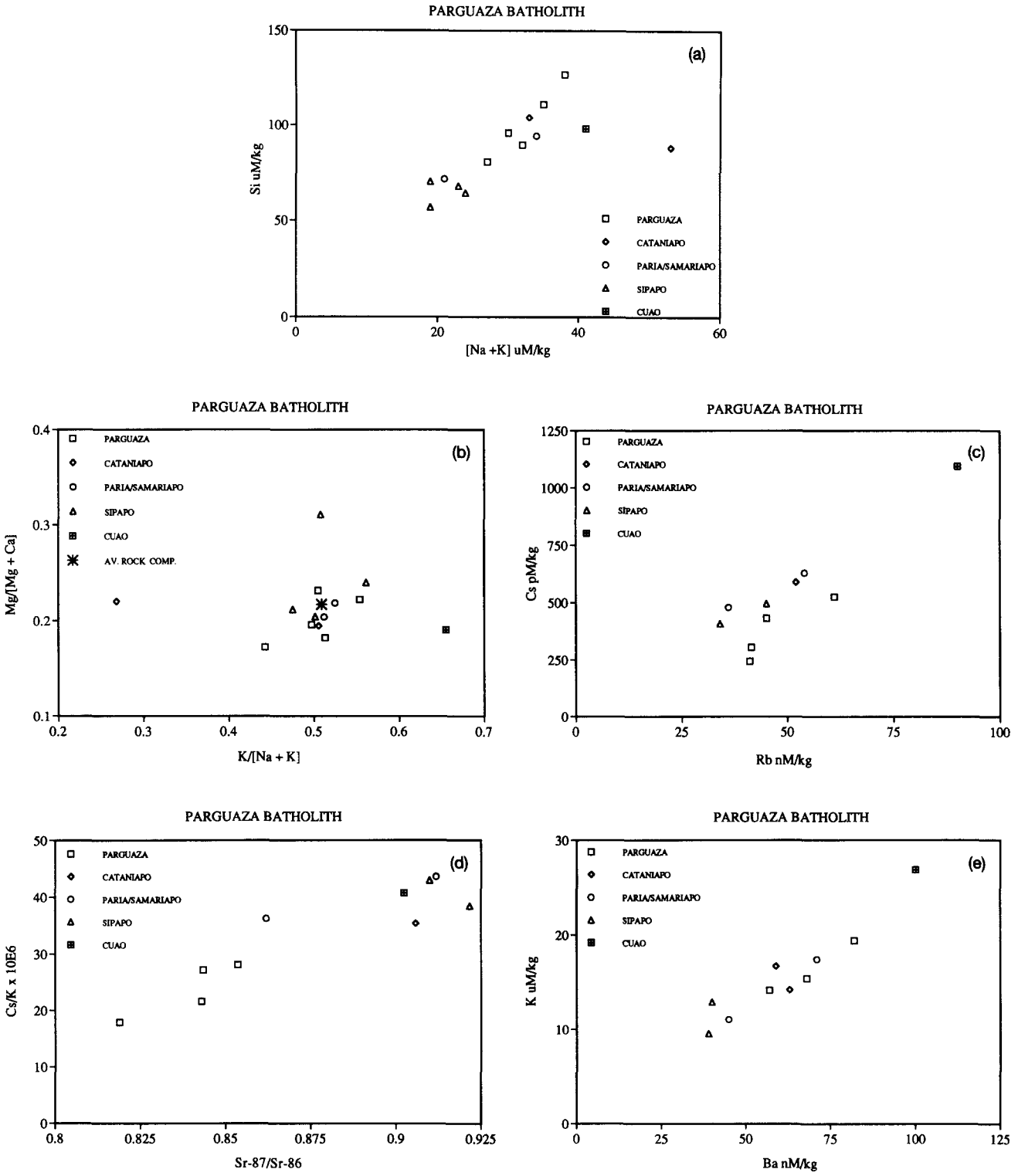

FIG. 7. (a–e) Property-property plots for the streams draining the Parguaza batholith.

of igneous and metamorphic rock types are present and that the region is one of the most lithologically diverse of any on the Shield (Sidder and Mendoza, 1991; Gibbs and Barron, 1993; USGS, 1993).

The rivers show a wide range in concentrations with TZ^+ ranging from ~20 to 340 μeq/kg (Table 2). Of the few pH measurements available only two are <6; however, the alkalinities are generally positive, precluding the extreme low pH values seen in the Parguaza drainage. The Si concentrations are quite high with most between 100 and 300 μM.

On the property-property diagrams (Fig. 9), the data form elongate trends indicative of lithologic heterogeneity. There

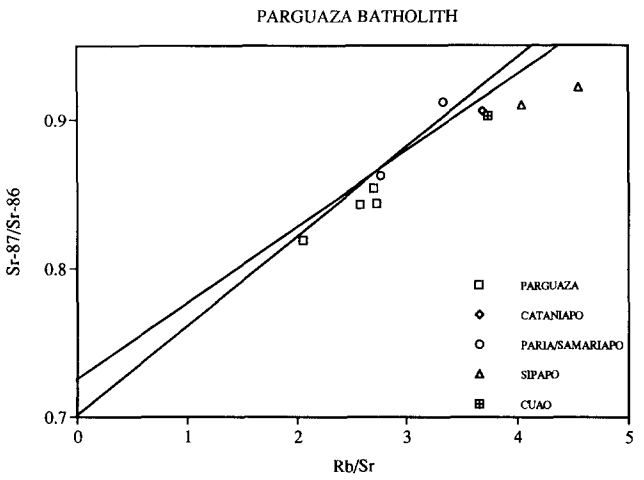

FIG. 8. The "fluvial isochron" for the Parguaza batholith. The stream data are compared with the published (recalculated) whole-rock isochrons for the batholith (solid lines). References are in the text.

is a good correlation between Si and (Na + K) with the intercept offset to slightly positive Si values, perhaps indicative of the dissolution of quartz or kaolinite. However, the ratio Si:(Na + K) is about 2.3, much lower than the value of over 3 seen in the Parguazan streams. Thus, some kaolinite is probably forming in these drainages in addition to the continued reaction to gibbsite. The data form a linear trend on the ternary cation diagram. The data from the upper Orinoco and the Rio Branco are among the most magnesian in the entire Shield. These must drain either unmapped exposures of the Roraima mafics or the tonalitic gneisses reported to be common in the region (Gaudette and Olszewski, 1985). There is no indication in the data from the Padamo, Ocamo, or the upper Orinoco of the presence of rapakivi granite in their headwaters in the Sierra Parima, as reported by Gaudette and Olszewski (1985). There is a reasonably good correlation between the heavy alkalis, Rb, and Cs. There is a tendency for the streams with the highest Cs/K ratios to have the most radiogenic Sr although the correlation is not as clear-cut as for the Parguazan drainages. The scatter may be due to secondary uptake of Cs or to the heterogeneous geology of the individual basins. The rivers are relatively enriched in Ba with the upstream Orinoco having a value of 288 nM. The correlation with K shows some scatter with an average ratio K:Ba ~ 200.

Gaudette and Olszewski (1985) reported whole-rock Rb-Sr data for samples collected along the Ventuari, Casiquiare, Padamo, and Upper Orinoco. They reported an average age of 1.75 b.y. Their isochrons are included in Fig. 9 along with the river data. All of the latter, with the exception of the Cunucunuma, fall on the isochrons, consistent with "complete" weathering. Taken overall, the intensity of weathering in the southwestern Shield, as characterized by the alkali-alkaline earth systematics and the Si:(Na + K) ratios, is slightly less severe than in the Parguazan terrain. While there is complete release of the cations, with the possible exception of Cs, some Si is held up, presumably as kaolinite. The lithologic heterogeneity of the region, as compared to the homogeneous Parguazan, is likely responsible for the higher scatter in the interelemental and isotopic correlations.

5.3. Lowland Shield

Of the rivers draining the lowland Shield, the Upper Negro-Guainia and the Atabapo in the extreme southwest are far

TABLE 2 CHEMICAL DATA FOR STREAMS DRAINING THE SOUTHWESTERN SHIELD

River name	sample number	date d/m/yr	Na uM/kg	K uM/kg	Mg uM/kg	Ca uM/kg	Cl uM/kg	SO_4 uM/kg	alkalinity ueq/kg	Si uM/kg	pH	$^{87}Sr/^{86}Sr$	Sr nM/kg	Rb nM/kg	Cs pM/kg
Orinoco ab Ventuari	146	13/06/82	17.9	11.8	3.5	6.0	3.6	0.6	18	77	5.3	-	-	-	-
	470	01/03/83	52.4	27.9	9.7	17.7	6.4	1.4	98	176	6.3	0.7415	186	-	-
Orinoco @ Guachapana	581	19/10/84	21.3	13.4	3.8	6.4	3.9	0.0	50	107	6.1	-	-	-	-
	766	15/05/86	22.8	14.8	4.8	6.9	0.0	0.0	30	85	-	-	-	-	-
Orinoco ab Casiquiare	476	04/03/83	79.2	37.2	18.0	32.4	8.5	1.5	182	248	6.6	0.7415	186	83	858
	583	07/10/84	49.4	28.4	18.5	19.1	6.9	0.0	109	175	-	-	-	-	-
Orinoco ab Ocamo	149	14/06/82	52.1	30.3	13.5	21.3	7.9	0.8	111	184	6.4	-	-	-	-
	588	18/10/84	152	37.2	19.3	31.9	16.5	4.9	236	221	6.7	-	-	-	-
Orinoco ab Platinal *	579	19/10/84	102	55.3	39.0	57.3	13.9	0.0	379	308	7.8	0.7304	381	97	567
Cunucunuma @ Tabicure	582	17/10/84	22.6	12.9	1.9	4.1	6.2	0.0	6	92	-	0.7932	20.1	37	677
Padamo	584	18/10/84	40.1	23.0	6.3	11.5	4.9	0.0	79	153	6.4	0.7596	60.9	55	685
Ocamo @ mouth	148	14/06/82	56.1	25.1	16.9	20.8	6.9	0.0	123	187	-	-	-	-	-
	585	17/10/84	66.2	28.8	15.1	23.3	4.9	0.0	132	191	6.5	0.7370	136	50	456
Ocamo @ Las Palmas	587	17/10/84	64.5	28.3	15.1	23.5	5.9	0.0	120	181	-	-	-	-	-
Pamoni	591	05/10/84	15.1	3.7	1.0	1.4	3.5	0.0	-32	36	-	0.7826	10.5	9.6	174
Pasiba @ mouth	592	"	28.1	18.7	2.7	5.3	3.2	0.0	33	108	-	0.7993	34.4	45	496
Siapa @ mouth	593	"	46.0	18.6	5.0	8.1	16.5	4.9	31	116	-	0.7486	61.7	42	440
Pasimoni @ mouth	594	"	16.6	3.7	1.6	2.1	2.2	0.0	-53	30	-	0.7430	13.5	7.9	118
Casiquiare @ Tama Tama	477	04/03/83	36.4	21.2	6.2	10.8	6.7	1.3	31	114	6.3	-	-	-	-
	590	06/10/84	51.8	29.9	12.2	19.8	5.6	0.0	117	176	-	-	-	-	-
Casiquiare @ Solano	595	05/10/84	21.7	12.5	4.0	6.3	4.2	5.6	3	79	-	-	-	-	-
Casiquiare @ S. Sebastian	142	13/06/82	13.3	10.0	3.0	5.0	3.6	0.4	-5	58	4.7	-	-	-	-
	596	05/10/84	22.4	13.2	4.0	6.4	5.6	4.9	-0.4	84	-	-	-	-	-
Branco @ mouth	BR1	08/77	62.0	24.3	21.7	24.7	15.5	3.0	128	191	6.6	0.7259	140	43	260
	BR2	04/78	85.0	30.1	40.8	44.2	16.0	2.7	252	192	6.7	0.7295	263	54	384
Ventuari @ mouth	145	13/06/82	26.5	14.6	6.4	9.8	3.8	0.6	49	109	6.0	-	-	-	-
	471	01/03/83	58.0	26.1	11.3	17.8	5.7	0.9	108	192	6.2	-	-	-	-
	540	18/10/84	32.5	15.3	7.1	9.6	5.3	0.0	62	117	6.0	0.7415	65.0	-	-
	761	14/05/86	47.9	16.2	5.0	8.3	9.6	0.0	42	98	-	-	-	-	-
Ventuari @ Kanaripo	541	19/10/84	29.4	14.8	6.8	9.2	3.5	0.0	54	110	-	-	-	-	-
Ventuari @ Cacuri	544	"	49.5	22.2	11.1	15.6	4.2	4.1	110	192	6.6	0.7255	117	39	480
Parucito @ S. Juan	543	"	76.1	25.1	14.3	18.9	7.6	0.0	141	179	6.5	0.7351	122	47	826

* Farthest upstream sample on the Orinoco main-stem.

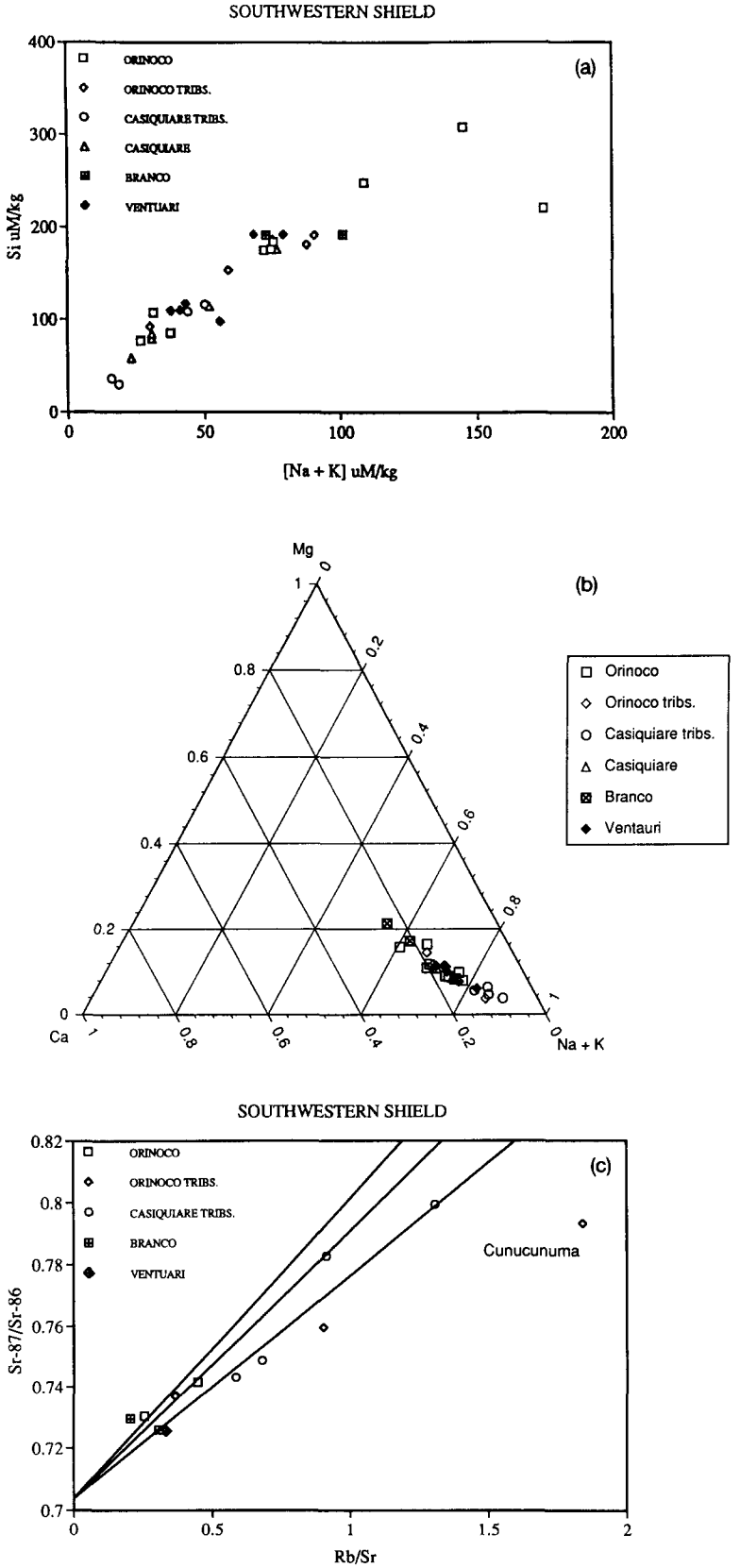

FIG. 9. (a–c) Selected property-property diagrams for the streams draining the Southwestern Shield.

removed from any Andean influence. Above the Branco, the Lower Negro receives the major right bank tributary, the Uaupes, which has headwaters in the Andean foothills. Farther north the left bank streams, the Inirida, the Tomo, and the Vichada, while not draining the Andes directly, are geographically contiguous to the Guaviare and the Meta, two of the major Andean rivers (Fig. 2). The course of the Inirida parallels that of the Guaviare across the lowlands and the two rivers join just above their confluence with the Orinoco. The Tomo and the Vichada drain the region between the northeastwards flowing Meta and the Orinoco. Their headwaters extend very close to the main channel of the Meta. Therefore, the possibility exists that these streams are also draining alluvial deposits of Andean origin or that they even receive water from the Andean rivers during overbank flow at high stage. The southern rivers drain only basement rocks formed during the Nickere metamorphic event at 1.3 b.y. (Priem et al., 1982). Basement outcrops also occur throughout the drainages of the northern rivers.

All these lowland streams are remarkable for their extreme dilution (Table 3). If protons are neglected, TZ^+ is always <50 μeq/kg and often <15 μeq/kg. The rivers are all acidic, most with pH < 5.5 and negative "alkalinities". In most of the streams, protons are the dominant cation. With such extreme compositions, the sea salt correction (Cl ranges from <1 to 12.7 μM) is very significant for Na and Mg. The Si concentrations range from 18 to 127 μM. The data form several groupings on the Si vs. (Na + K) diagram (Fig. 10). The samples from the southern rivers (Atabapo, Guainia, Negro) define a trend with slope of $\sim$3.8 that passes through the origin, indicative of gibbsite formation. The data from the Inirida show no covariance of Si with the alkalies; the Si concentrations are quite uniform at around 70 μM. The Tomo and Vichada have very high Si values as compared to their cation concentrations. The alkali-alkaline earth diagram shows broad scatter. The Negro-Guainia samples fall on or slightly above the igneous differentiation trend and the Atabapo data fall on or below it. The Inirida data scatter widely above the trend. The Tomo and the Vichada show similar behavior consistent with continued reaction of partially degraded detrital material of Andean origin stored in their flood plains. On the ternary cation diagram the southern rivers fall on or slightly below the igneous differentiation trend as exhibited by the datasets from the other sub-basins (Fig. 10). The sample from the Tomo also falls on this trend. The data from the Vichada and (with one exception) the Inirida fall markedly above the trend, towards the Mg apex. This overall pattern is consistent with the inferred reworking of partially degraded Andean detritus. There is no obvious explanation for the one Inirida point that falls to high Ca. It was collected at high rising stage and has a positive alkalinity and appreciable amounts of sulfate as compared to the other samples. This may indicate some contribution of water from the Guaviare.

The dataset defines a tight relationship between Rb and K; however, there is no relationship between Rb and Cs or Ba and K. The single data points from the Guainia and the upper Negro fall on the whole-rock isochron reported by Priem et al. (1982) for the gneisses and granites in its drainage (Fig. 10). All the other rivers fall below this line. While this might be expected for the northern rivers, the substantial deviations shown by the lower Negro and especially the Atabapo are strongly at variance with the reported whole-rock data from their drainages (Priem et al., 1982; Gaudette and Olszewski, 1985). Given the regularity of the Rb:K relationship, it is difficult to ascribe this to chemical fractionation processes during weathering or to secondary adsorption of Rb. The extremely dilute nature of these rivers, particularly for Ca, and the magnitude of the deviations rule out admixture of Andean waters as an explanation.

The generally low concentrations, especially of Si, and the high acidity indicate that these streams are interacting with a severely weathered substrate. Despite the inconsistencies in the Rb-Sr data and the unconstrained possibility of exchange of water with the Andean tributaries it is clear that the rivers of the lowland Shield represent an extreme example of transport-limited weathering (Stallard and Edmond, 1983).

5.4. Suapure/Manapiare Basins

The Suapure and Manapiare flow north and south respectively, approximately along the eastern contact of the Parguazan batholith with the Pacariama-Cuchivero Formation. Thus they receive affluents both from the batholith and from the volcano-plutonic terrain to the east. In addition, they drain

TABLE 3 CHEMICAL DATA FOR STREAMS DRAINING THE LOWLAND SHIELD

River name	sample number	date d/m/yr	Na uM/kg	K uM/kg	Mg uM/kg	Ca uM/kg	Cl uM/kg	SO_4 uM/kg	alkalinity ueq/kg	Si uM/kg	pH	$^{87}Sr/^{86}Sr$	Sr nM/kg	Rb nM/kg	Cs pM/kg
Atabapo	151	14/06/82	3.3	1.9	0.7	1.3	1.7	0.3	-44	18	4.3	-	-	-	-
	303	17/11/82	4.7	0.8	0.6	1.1	1.7	0.3	-61	30	4.2	-	-	-	-
	473	02/03/83	12.0	3.2	1.1	2.5	2.8	0.3	-29	48	4.4	-	-	-	-
	545	19/10/84	12.8	0.8	0.9	1.0	0.0	0.0	-45	24	-	-	-	-	-
	608	26/05/85	8.9	4.9	0.9	1.5	6.3	0.0	-63	29	4.5	0.7461	9.9	14	259
Inirida	180	25/06/82	8.4	6.0	6.3	12.7	4.9	3.3	16	67	5.2	-	-	-	-
	301	17/11/82	6.1	4.4	3.7	2.1	4.2	2.1	-21	77	4.5	-	-	-	-
	474	03/03/83	6.5	5.6	2.9	1.7	4.2	2.1	-16	73	4.2	-	-	-	-
	546	19/10/84	6.2	4.7	4.0	3.6	3.5	0.0	5	66	-	0.7227	18.1	11	63
	609	26/05/85	7.3	11.0	5.1	3.3	5.9	0.0	-20	75	5.4	0.7247	20.1	18	174
Vichada	548	17/10/84	11.8	8.5	2.3	1.7	7.0	0.0	10	91	-	-	-	-	-
	602	24/05/85	13.2	17.2	1.6	2.0	12.4	0.0	48	127	6.1	0.7139	10.9	31	165
Tomo	613	31/05/85	13.6	7.4	2.1	2.0	12.7	0.0	-10	114	6.3	0.7186	16.1	19	244
Guainia ab Casiquiare	143	13/06/82	3.8	2.9	1.2	1.8	1.5	0.3	-39	25	4.3	-	-	-	-
	478	04/03/83	13.9	8.1	2.0	2.6	2.8	0.6	-20	65	4.7	-	-	-	-
Guainia @ Catanccuname	597	01/05/84	5.9	2.6	1.1	1.5	2.8	0.0	-36	81	-	0.7543	8.0	6.5	174
Negro @ S. Carlos	598	10/05/84	17.4	8.3	2.9	4.8	3.5	0.0	-14	64	-	-	-	-	-
Negro ab Branco	UN1	08/77	10.4	7.9	3.2	5.2	7.6	2.3	-16	64	4.8	0.7195	30.2	15	354
	UN2	04/78	13.5	6.6	2.6	4.2	7.0	2.0	-5	57	4.6	0.7378	24.8	15	280

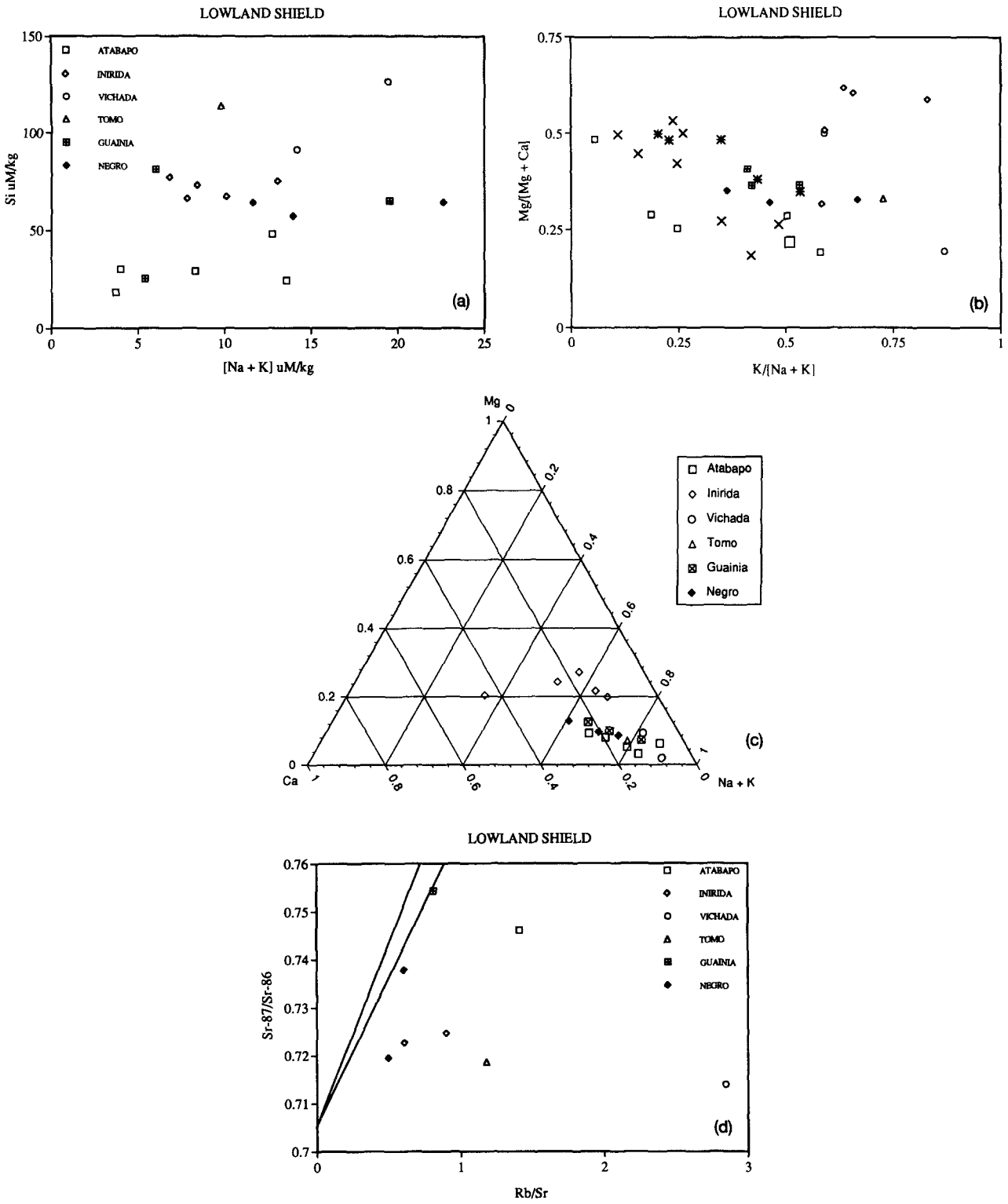

FIG. 10. (a–d) Selected property-property diagrams for the rivers draining the Lowland Shield. On the alkali-alkaline earth diagram the compositions of rocks from the Imataca Complex (×) and the Parguaza batholith (□) are shown along with those for average igneous rocks (*).

scattered outliers of the Roraima. The Manapiare meanders across an alluvial plain with minor outcrops of the Trans-Amazonian basement before joining the Ventuari below San Juan.

These rivers (Table 4) are only slightly acidic (pH > 6, alkalinity between 60 and 85 μeq/kg) and have intermediate Si concentrations (109–170 μM). The ratio Si:(Na + K) is about 2 and the data fall in intermediate positions on the ig-

TABLE 4 CHEMICAL DATA FOR THE SUAPURE AND MANIAPIARE

River name	sample number	date m/d/yr	Na uM/kg	K uM/kg	Mg uM/kg	Ca uM/kg	Cl uM/kg	SO_4 uM/kg	alkalinity ueq/kg	Si uM/kg	pH	$^{87}Sr/^{86}Sr$	Sr nM/kg	Rb nM/kg	Cs pM/kg
Suapure	311	24/11/82	53.2	23.6	7.5	11.6	7.6	1.1	84	170	6.6	0.7625	55.1	47	236
	460	06/03/83	44.1	34.2	10.3	17.0	13.3	2.0	78	137	6.5	0.7656	90.1	77	449
	528	13/10/84	48.9	21.0	6.8	10.4	2.7	0.0	85	156	6.4	-	-	-	-
Manapiare ab S.Juan	542	18/10/84	34.5	15.1	5.7	7.5	3.5	0.0	60	109	5.9	0.7452	45.3	30	118

neous differentiation trends on the cation diagrams. The Rb/K and Cs/Rb ratios are distinctly different from those in the streams that drain the Parguazan batholith exclusively. The high Rb in the samples (30–77 nM) probably reflects a granitic source as does the relationship between Cs/K and $^{87}Sr/^{86}Sr$. The lower Cs values (118–449 pM: 10^{-12} mol/kg) may indicate depleted sources or uptake by the sediments of the relatively extensive flood plains of both rivers. The three river data points fall between the reported isochrons for the Parguazan and Cuchivero granites and for the Roraima volcanics, confirming the severity of the weathering.

5.5. Cuchivero/Caura Basins

The Caura and Cuchivero drain the volcano/plutonic rocks of the Pacaraima-Cuchivero Formation. In its headwaters, the Caura drains the Imataca and Uatuma terrains and minor outcrops of the Roraima. The Tortuga, a smaller stream to the west, drains similar rocks to the Cuchivero as does the Paracitu, a tributary of the Ventuari to the south. Both the Tortuga and Paracitu have quite extensive flood plains in their meandering lower courses, a relatively unusual feature for the Shield rivers.

The rivers in these basins (Table 5) have intermediate dissolved loads (TZ^+ in the range 70–220 μeq/kg) and are only weakly acidic (pH > 6, alkalinity > 50 μeq/kg). The Si values vary from ~100 μM to over 230 μM. On the Si-(Na + K) diagram the six samples from the Caura give a tight straight line that extrapolates to the Si axis at a value of ~30 μM (Fig. 11). The Si:(Na + K) ratio is 2, much lower than observed to the west and indicative of kaolinite production. The data from the Cuchivero are more scattered but define a trend with a ratio of ~1.9 that extrapolates to the origin. The Paracitu and Tortuga fall on the Cuchivero trend. The plot of the alkali-alkaline earth ratios follows the igneous differentiation trend with no discernible cation fractionation. Thus, weathering is complete for the major cations. The Na/Rb and Na/Cs ratios are distinctly higher than in the Parguazan and southwestern Shield rivers. The Tortuga has a very low Cs concentration resulting in a high Na/Cs ratio. Most of the Tortuga's drainage lies in recent sediments and these probably take up Cs in preference to the lighter alkalies. The interelement correlations are relatively poor and there is no covariance of Cs/K with the strontium isotopes. This again suggests that weathering is significantly less intense than in basins to the west. The Ba data do not define a trend with K but fall in a restricted range with a ratio K:Ba ~175.

The whole-rock isochrons for a number of the formations within the drainage are plotted in Fig. 11 (Montgomery and Hurley, 1978; Gaudette et al., 1978; Gaudette and Olszewski, 1985). The rivers have a very narrow range of $^{87}Sr/^{86}Sr$ ratios that, while falling between the isochrons, do not themselves define a trend. The exception is the Tortuga which falls well to the right. This may reflect the presence in its flood plain of sediments of Andean origin derived from the Orinoco main stem during periods of high inundation. The generally low $^{87}Sr/^{86}Sr$ ratios in the waters may be partially a reflection of the presence of more basic rock types; however, the lack of a clear correlation between the isotope and Rb/Sr ratios are further indications of relatively less intense weathering than to the west.

5.6. Aro Basin

The Aro and its tributaries drain the Imataca Complex and the greenstone terrain lying to the east. Included in this section are the Tiquire, Orocopiche, and Pao, small tributaries adjacent to the Aro and draining the same rock types.

The rivers show a wide range in concentrations (TZ^+ from ~30 to >550 μeq/kg) with silica values as high as 455 μM

TABLE 5 CHEMICAL DATA FOR CUCHIVERO, CAURA AND ADJACENT STREAMS

River name	sample number	date d/m/yr	Na uM/kg	K uM/kg	Mg uM/kg	Ca uM/kg	Cl uM/kg	SO_4 uM/kg	alkalinity ueq/kg	Si uM/kg	pH	$^{87}Sr/^{86}Sr$	Sr nM/kg	Rb nM/kg	Cs pM/kg
Cuchivero	163	20/06/82	58.3	24.3	15.5	21.1	9.1	0.0	122	170	6.8	-	-	-	-
	320	01/12/82	84.6	24.8	23.1	30.3	12.2	1.7	181.	233	7.0	0.7397	124	44	331
	455	04/03/83	63.2	34.4	17.3	23.8	23.6	2.6	118	170	6.9	0.7367	118	62	527
	520	09/10/84	84.6	22.2	20.6	26.7	11.2	0.0	176	213	6.6	0.7436	109	47	409
	619	07/06/85	58.4	22.2	11.7	16.1	16.5	0.0	85	116	6.3	-	-	-	-
	723	27/03/86	92.8	25.7	24.5	34.9	15.0	0.0	205	239	5.7	-	-	-	-
	826	23/06/87	57.7	27.2	15.0	21.4	9.2	3.0	119	170	6.0	-	-	-	-
Caura bel Tiquire	165	21/06/82	33.7	14.6	7.7	11.9	6.3	0.2	57	123	6.3	-	-	-	-
	211	20/08/82	30.9	14.6	8.2	12.0	7.5	0.3	50	109	6.2	-	-	-	-
	322	02/12/82	53.5	18.4	10.6	16.2	8.7	1.3	88	178	6.9	0.7323	84.3	28	252
	454	03/03/83	69.8	23.3	12.2	17.3	13.1	1.0	111	209	7.2	-	-	-	-
	519	08/10/84	40.9	17.3	5.5	14.1	15.5	1.1	77	136	6.3	0.7350	75.3	30	299
	621	07/06/85	26.2	16.9	7.8	10.0	8.4	0.0	65	98	6.5	-	-	-	-
	702	27/03/86	65.8	21.1	14.7	21.7	10.9	0.0	127	198	5.8	-	-	-	-
	712	"	64.5	21.2	14.7	22.5	9.7	0.0	132	197	5.8	-	-	-	-
	733	"	64.7	20.6	14.3	22.5	7.6	0.0	126	194	5.8	-	-	-	-
	795	15/05/86	31.5	14.9	8.6	7.6	6.8	0.0	124	107	6.1	-	-	-	-
Tortuga bel Maniapure	314	26/11/82	61.3	19.4	5.6	9.7	12.5	0.1	75	153	5.9	0.7531	33.2	37	103

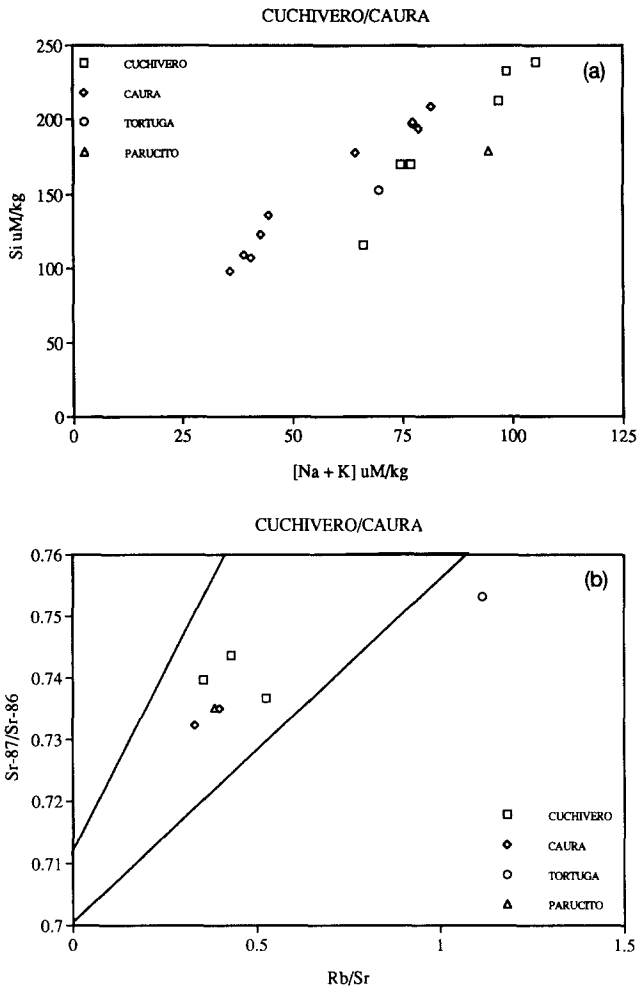

FIG. 11. The Si-alkali diagram (upper) and the strontium isotopic systematics for the Cuchivero-Caura.

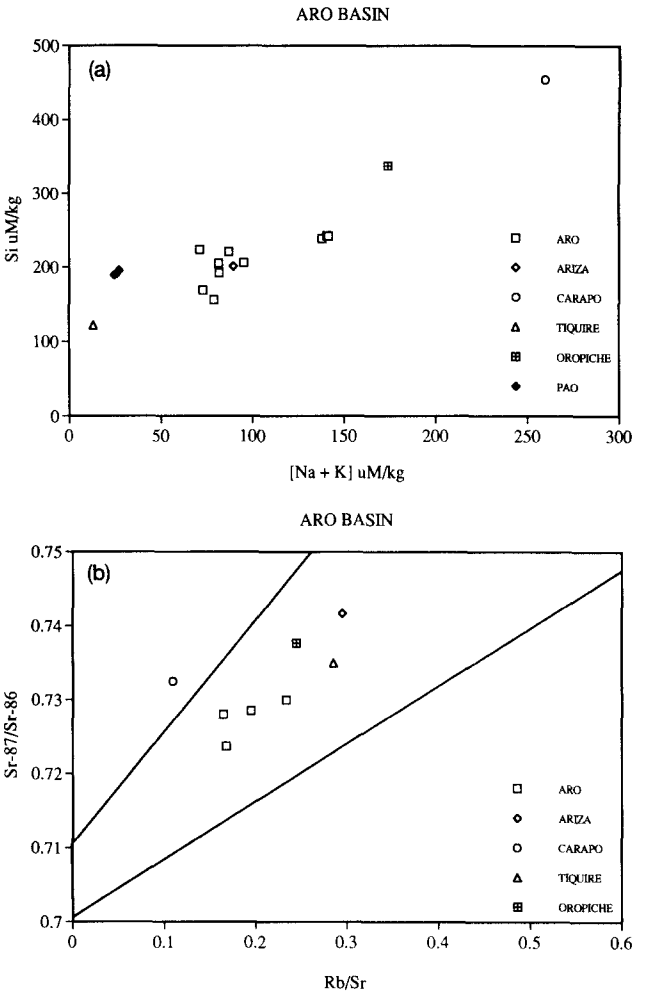

FIG. 12. The Si-alkali diagram (upper) and the strontium isotopic systematics for the Aro drainage.

(Table 6); in general, the concentration values are higher than those from rivers to the west. The larger streams are quite alkaline with pH > 6.5 and alkalinities up to 545 μeq/kg. On the alkali-Si diagram (Fig. 12), the data follow a well-constrained trend with Si:(Na + K) of 1.3 and a Si axis intercept of ~100 μM. On an alkali-alkaline earth ratio plot, the data for the Aro fall towards the basic end of the igneous rock trend. However the Carapo, Ariza, Oropiche, and Tiquire have more extreme compositions with Mg/(Mg + Ca) as high as 0.48 and K/(Na + K) down to 0.15 and lower. These values are close to those reported by Dougan (1977) for the amphibolites and mafic granulites of the Imataca Complex which these rivers drain. The very high Na and K concentrations in the Carapo and Oropiche are coupled with high Rb

TABLE 6 CHEMICAL DATA FOR THE ARO DRAINAGE AND ADJACENT STREAMS

River name	sample number	date d/m/yr	Na uM/kg	K uM/kg	Mg uM/kg	Ca uM/kg	Cl uM/kg	SO_4 uM/kg	alkalinity ueq/kg	Si uM/kg	pH	$^{87}Sr/^{86}Sr$	Sr nM/kg	Rb nM/kg	Cs pM/kg	Ba nM/kg
Aro @ mouth	114	03/06/82	78.5	21.2	27.9	31.0	20.9	0.0	163	205	7.1	0.7300	137	32	174	-
	324	04/12/82	88.4	19.8	33.2	37.3	24.2	1.9	200	221	7.3	0.7280	176	29	244	186
	452	02/03/83	78.3	16.8	29.2	29.9	27.3	5.8	156	224	7.4	0.7285	159	31	221	175
	516	06/10/84	94.3	19.9	27.6	29.0	21.6	2.8	181	206	6.8	-	-	-	-	172
Aro @ bridge	501	02/10/84	85.4	18.7	22.5	30.1	25.6	0.0	174	192	6.8	-	-	-	-	166
	703	15/03/86	138	32.9	53.9	49.2	34.5	0.0	322	243	-	-	-	-	-	228
	706		138	33.0	54.0	49.0	33.5	0.0	331	242	-	-	-	-	-	-
	732		137	32.5	52.8	50.6	36.0	0.0	313	239	-	-	-	-	-	-
	739		139	34.2	53.3	50.4	36.7	0.0	318	242	-	-	-	-	-	-
Aro ab Carapo	555	23/10/84	71.9	11.9	22.0	27.8	12.7	0.0	161	169	-	-	-	-	-	155
Aro ab falls	556	"	65.8	22.5	19.9	26.4	11.0	0.0	132	156	-	0.7237	137	23	181	171
Ariza	553	"	81.3	21.4	25.8	26.8	15.1	0.0	171	201	-	0.7417	115	34	252	189
Carapo	554	"	250	34.5	78.6	82.7	29.1	0.0	545	455	-	0.7325	347	38	71	419
Tiquire	534	08/10/84	20.5	2.9	3.8	4.3	11.6	0.0	18	122	5.4	0.7350	20.3	5.8	142	37
Oropiche	502	01/10/84	174	37.8	38.3	36.5	43.2	5.6	252	338	5.3	0.7377	151	37	90	369
Pao near Caura	709	"	30.5	7.0	9.9	13.1	13.6	0.0	45	190	-	-	-	-	-	113
	727		30.2	8.5	9.7	12.8	16.3	0.0	55	189	-	-	-	-	-	-
	737		31.0	6.7	9.8	12.7	12.2	0.0	53	195	-	-	-	-	-	-

TABLE 7 CHEMICAL DATA FOR THE CARONI DRAINAGE

River name	sample number	date d/m/yr	Na uM/kg	K uM/kg	Mg uM/kg	Ca uM/kg	Cl uM/kg	SO_4 uM/kg	alkalinity ueq/kg	Si uM/kg	pH	$^{87}Sr/^{86}Sr$	Sr nM/kg	Rb nM/kg	Cs pM/kg
Caroni @ Ordaz	169	25/06/82	18.0	8.5	6.2	8.5	7.1	0.3	22	72	5.8	-	-	-	-
	210	23/08/82	18.8	7.9	6.2	8.3	6.0	1.0	19	78	6.4	-	-	-	-
	327	06/12/82	21.3	9.6	7.0	10.3	6.9	1.2	21	85	6.3	0.7322	37.6	13	47
	450	03/10/83	23.9	7.9	7.9	10.6	7.1	1.2	22	95	6.5	-	-	-	-
Caroni @ Guri	513	"	20.8	6.8	5.0	5.8	9.1	0.0	20	75	4.9	-	-	-	-
Caroni @ Capaura	503	02/10/84	16.0	8.9	4.4	7.2	7.7	0.0	18	77	5.6	0.7417	25.8	11	87
Antabare @ Arekuna	512	03/10/84	24.3	3.1	19.3	13.6	14.3	0.0	50	78	5.9	0.7198	38.4	5.6	109
Carrao@ Canaima	509	"	25.0	4.8	5.2	6.1	18.8	0.0	0.6	48	4.9	0.7341	17.5	6.5	78
Cucurital	511	"	7.3	4.8	2.6	4.1	4.9	0.0	-0.5	46	4.8	0.7393	17.3	6.7	63
Trib of Cucurital	510	"	22.5	9.2	7.7	10.2	7.0	0.0	47	102	6.0	0.7355	39.3	14	127
Uriman ab Uriman	504	02/10/84	11.6	7.1	2.9	4.3	5.6	0.0	37	62	5.0	0.7337	24.9	9.3	110
Yuruman @ S. Ignacio	507	"	24.0	12.5	2.1	4.2	6.3	0.0	33	111	6.2	0.7367	33.4	16	110
Paragua ab La Paragua	508	"	27.7	9.8	6.0	8.5	6.7	0.0	39	112	5.8	0.7326	43.0	-	-
Paragua ab Karun	506	"	26.8	12.3	6.5	9.8	6.3	0.0	37	107	5.6	0.7321	34.4	16	110
Karun ab Paragua	505	"	27.6	12.6	4.8	7.3	4.9	0.0	42	120	6.1	0.7349	34.6	16	126

and Ba but very low Cs. The data appear contradictory in that the high concentrations of dissolved species argue for intense weathering of generally basic rocks, whereas the high Na/Rb and Na/Cs ratios indicate extensive fractionation of the heavier alkalis into secondary weathering products. Based on the available geologic information, the rock types in the drainages of the Carapo and Oropiche are similar to those in the rest of the Complex, e.g., the Ariza. However, their courses lie within major fault zones. It appears that rapid weathering of cataclastic rocks in these zones and, perhaps, deeper circulation of groundwaters lead to partial weathering and the formation of secondary clay minerals that retain Cs and, to a lesser extent, Rb. Barium is enriched relative to the other streams which define a K:Ba ratio of ~135. The rest of the rivers in the basin show very similar alkali ratios suggestive of intense weathering.

Isochrons from the Imataca Complex and from some younger intrusive granites (Montgomery and Hurley, 1978) are plotted in Fig. 12, together with the fluvial data. The latter form a trend parallel to and between the rock isochrons. However, the Carapo falls to lower Rb values probably reflecting the secondary uptake referred to above.

The Aro was sampled close to its confluence with the Orinoco in June and November 1982 and March 1983. The $^{87}Sr/^{86}Sr$ ratios vary only from 0.7300 to 0.7280 and are correlated with changes in the Rb/Sr ratio. The sample with the highest isotope ratio has the highest Cs/K. Hence, as for the Parguaza, changes in the river chemistry reflect changes in the relative contributions from the different source areas rather than seasonal changes in the intensity of weathering. The data overall are consistent with a progressive eastwards decrease in weathering intensity and an increasing preponderance of basic rocks.

5.7. Caroni Basin

The Caroni is the easternmost sub-basin of the Shield drainage to the Orinoco. Its lower reaches are impounded by the huge Guri hydroelectric complex and the smaller dam at Macagua, the only artificial constrictions of any kind on the Shield rivers. Only minor affluents enter the Guri reservoir and the lower Caroni. Its major left-bank tributary, the Paragua, joins the main stem just above the Guri. The drainage of the Caroni lies almost entirely in the Roraima quartzite and the associated mafic intrusions (Briceño and Schubert, 1990; Briceño et al., 1991). The outcrop boundary of the Uatuma Supergroup volcanics marks the western watershed of the basin with only minor streams contributing to the Caroni from this terrain. Of the sub-basins sampled, the Antabare and the Cucurital and its (unnamed) tributary drain the tepuys of the Roraima Formation; the other streams also drain exposures of the mafic members. The Paragua and its major tributary, the Karun, drain the Uatuma terrain in addition to receiving inflows from the Roraima. The headwaters of the Paragua (above the Karun confluence) lie entirely in the Uatuma while those of the Karun also drain mafic Roraima rocks. There are large exposures of Roraima quartzites in the lower part of the basin.

The streams of the Caroni are among the most dilute in the upland Shield with TZ^+ between 20 and 80 μeq/kg (Table 7). Most of the rivers are "black" with pH between 4.8 and 6.5 and alkalinities between zero and 50 μeq/kg. The Si concentrations are generally less than 100 μM except in the Paragua/Karun drainage where they range up to 120 μM (Fig. 13). The data show a good correlation between Si and (Na + K) with a ratio of 2.5 and an Si intercept at 25 μM. On the alkali-alkaline earth plot and on the ternary cation diagram the data fall on the igneous differentiation trend. The extreme compositions are from the Antabare and the Uriman. The former is extremely mafic indicating intense weathering of (unmapped) Roraima basalts. The Uriman has a composition comparable to rivers draining the Parguaza batholith, although only the Roraima is mapped in its basin. The other data cluster at intermediate values such as would be produced by the weathering of detrital feldspars in the Roraima quartzite to kaolinite (Reid and Bisque, 1975; Briceño and Schubert, 1990). The rivers of the Caroni basin have the lowest alkali concentrations observed on the Shield. They also have higher Na/Rb and Na/Cs ratios than the other drainages. However the correlation between the alkali element ratios is much weaker than observed elsewhere and there is no relationship between Cs/K and $^{87}Sr/^{86}Sr$. The K/Ba data show a rough correlation with a ratio of ~150.

The whole-rock isochron obtained by Gaudette and Olszewski (1985) for the mafic intrusions of the Roraima is plotted in Fig. 13 along with the river data. The latter scatter about the whole-rock line. The samples from the Paragua and Karun fall significantly to the right as does one of the Caroni

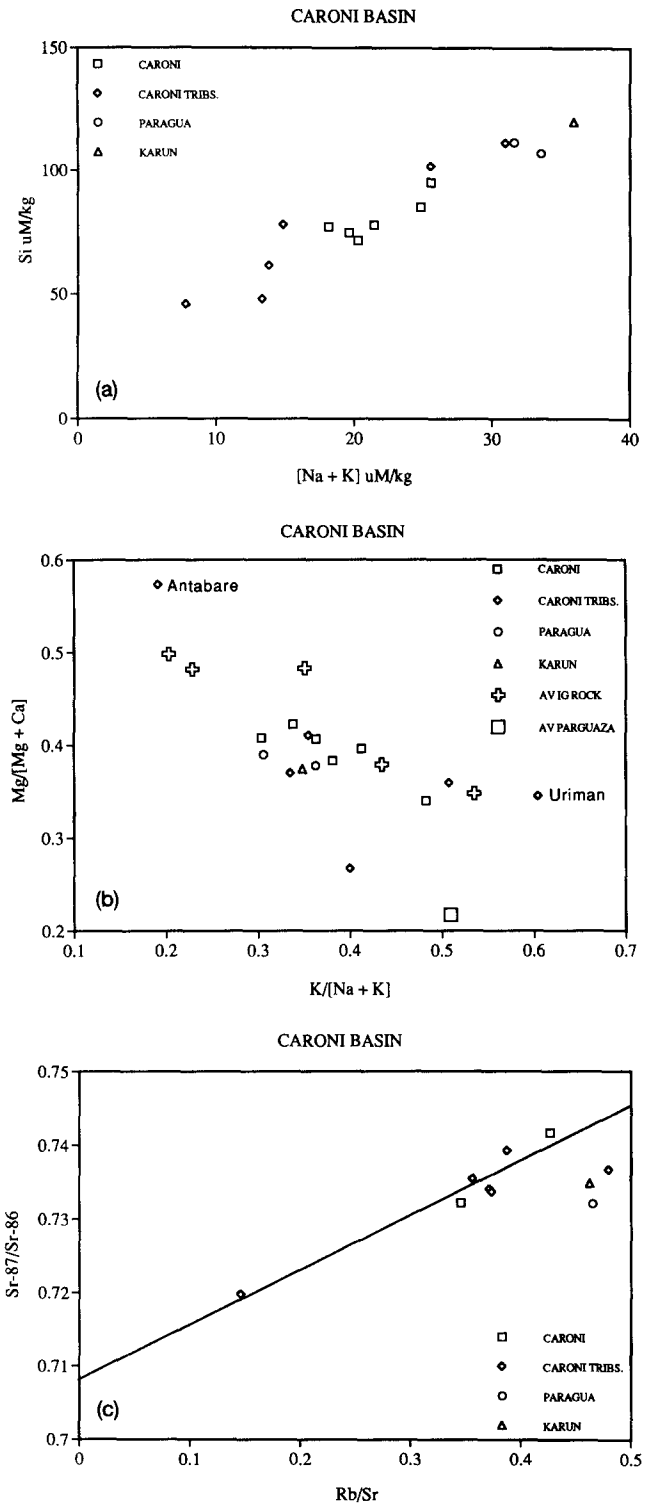

FIG. 13. (a–c) Selected property-property diagrams for the Caroni drainage.

tributaries. This may reflect inputs from local exposures of the 1.3 b.y. Nickerie granite. The range in isotopic composition of the river data is narrow (0.7198–0.7417) and much less radiogenic as compared to the whole-rock data (0.7321–0.8378), strongly suggesting that weathering has been only partial with Ca/Na-feldspars being destroyed in preference to the more resistant, high Rb/Sr minerals, the K-feldspars and mica.

6. THE DENUDATION RATE OF THE GUAYANA SHIELD

The present dataset for the dissolved load of the rivers of the Guayana Shield can be combined with information on the discharge and suspended load (Meade et al., 1990a) to produce estimates of the chemical and mechanical weathering yield. While the hydrologic data are seasonally representative and often extend over a decade for a particular tributary, the dataset for the concentrations of dissolved and suspended material is restricted to that presented here, save for previously reported work on the Caura (Lewis et al., 1987). While all the major streams have been sampled on several different occasions, there is nothing resembling a detailed time-series. As already pointed out, the flood crest is markedly undersampled (Fig. 3). Where data exist, there is seen to be a significant inverse relation between concentration and discharge (see also; Lewis et al., 1987). Thus, the estimates of the denudation rates are probably high, since they combine annual average discharges and suspended loads with estimates of the average dissolved load largely based on samples from falling, low, and rising stages, i.e., from October through June.

The data used in the calculations are summarized in Table 8. The striking result, given the above caveat, is that the erosion rates are very low; the combined mechanical and chemical weathering fluxes are equivalent to an average areal erosion rate of between ten and twenty meters per million years in the eastern and central upland Shield to values of around five in the western lowlands (cf. data in Saunders and Young, 1983). There is exact agreement between these calculations and those of Lewis et al. (1987) for the Caura. Since the latter are based on much more detailed sampling, the uncertainties discussed above for the other drainages are probably not severe. To put these denudation rates in some perspective, the accumulation rate of oceanic, largely aeolian, detrital sediments in deep basins remote from the continents is about one meter per million years.

The extremely low denudation rates are consistent with recent determinations of cosmogenic exposure ages for the quartzite erosion surface atop Mount Roraima on the Venezuelan-Brazilian border ($\sim$1 m My^{-1}; Brown et al., 1992), given the uncertainties in both types of estimation and the differing rock types, and for outcropping quartz veins in laterite on the West African Craton in Burkina Faso (3–8 m My^{-1}; Brown et al., 1994). Data on the ages of meteorite craters on the Yilgarn Block in Southwestern Australia suggest denudation rates of 1–2 m My^{-1} (Shoemaker et al., 1990). Geochemical mass balances for the drainages in the basin of Lake Chad give rates of $\sim$8 m My^{-1} (Gac, 1980).

In general, the dissolved and particulate weathering fluxes in the Shield rivers are of comparable magnitude; however, a major proportion of the dissolved load is silica. In moles per equivalent, [Si:TZ$^+$], the lowland Shield rivers give values around 3.0, those draining the Parguazan batholith about 2.0, and the high Shield areas between 1.5 and unity. This is in general accord with the estimates of weathering intensity as the values for average acidic rock types (ignoring normative quartz) range between 3 and 4 (Table 9). The data for the

TABLE 8 DENUDATION RATE OF THE GUAYANA SHIELD

RIVER	DRAINAGE AREA 10^3 km^2	DISCHARGE 10^3 m^3 sec^{-1}	Na	K	Mg	Ca	Si	Susp. Load mg kg^{-1} *	Dissolved flux 10^9 mol yr^{-1}	Dissolved Flux ** mg cm^{-2} yr^{-1}	Particle Flux 10^9 gm yr^{-1}	Particle Flux mg cm^{-2} yr^{-1}	Denudation *** meters m.y.$^{-1}$	Si:TZ$^+$ mol:eq
			«		uM/kg*		»							
ORINOCO @ Ventuari	60	4.0	21	15	5.5	10	100	7	19	1.6	88	1.5	12	1.5
VENTUARI	40	3.0	31	19	8.5	11	130	10	25	2.4	94	2.4	19	1.5
ATABAPO	10	0.40	5.3	2.0	0.60	1.5	30	3	0.12	0.25	4	0.36	2.4	2.6
GUAINIA @ S. Carlos	26	2.3	5.3	4.0	1.3	2.0	50	4	0.90	0.94	29	1.1	8.0	3.1
PARGUAZA	5.4	0.40	15	16	1.1	4.5	105	20	2.3	1.7	25	4.8	10	2.5
CUCHIVERO	18	0.32	65	25	17	23	180	60	3.1	0.81	60	3.4	17	1.1
CAURA	50	2.7	32	17	9	14	140	15	18	1.8	130	2.6	18	1.5
ARO	14	0.27	69	20	28	33	220	30	3.1	1.1	26	1.8	12	1.1
CARONI	93	4.1	14	8.0	6.5	9.0	80	10	15	0.83	130	1.4	9.0	1.5

* Flow weighted, seasonally averaged data. ** Mass flux for Si calculated as SiO_2. *** Mean rock density taken as 2.5 gm cc^{-1}.

minor alkalies and the Rb/Sr isotopic systematics suggest that the basement rocks are undergoing dissolution to leave an essentially cation-free residue of quartz, gibbsite, kaolinite, and Fe oxyhydroxides. A thermodynamic analysis of the data, using Mg as the most refractory cation (Fig. 14), shows that all samples fall in the kaolinite stability field. The severity of weathering can be appreciated by noting that the global average value of the [Si:TZ$^+$] ratio attributed to silicate weathering is ~0.4 (Holland, 1978). Thus, intense weathering of stable Shields to kaolinite and gibbsite results in a substantial fluvial flux of silica unaccompanied by significant increments in the cations and, therefore, alkalinity. In fact, the Shield rivers contribute about half of the total Si transported by the Orinoco (J. M. Edmond, unpubl. data); they also contribute ~40% of the K indicating the relative differences in weathering severity between the Andes and the Shield. They have negligible importance for the other species. A closely similar proportionality exists between the Andean and lowland tributaries of the Amazon (Stallard and Edmond, 1983).

The areal denudation rates conceal the actual erosion mechanisms. In the Roraima terrains of the eastern Shield, it is by karst-like dissolution of the quartzite and by slope retreat in the incised river valleys (Briceño and Schubert, 1990; Briceño et al., 1991). Farther west, the Roraima has been largely removed and the regional uplift has resulted in the partial stripping of the lateritic cover and the exposure of inselbergs of basement rock. Onion-skin weathering is common on these smooth rounded surfaces. However, due to the strong seasonality of the precipitation and the high temperatures, the exposures are wet only a very small proportion of the time. Thus, weathering remains very slow. In the buried depressions in the basement topography in this region and over most of the Lowland Shield, the site of weathering is in the transition zone or "etching front" between the lateritic mantle and the pristine basement rocks, an environment that is likely to be permanently waterlogged and with a very low hydraulic gradient (Twidale, 1982, 1990). The combination of differing factors in these environments results in a relatively uniform and very low rate of denudation.

The dissolved flux from the various terrains on the Shield is a measure of the penetration rate of the weathering front into the unreacted substrate. From the data in Table 9, the weathering of 100 moles of average Shield rocks to kaolinite produces 16.9 moles of dissolved cations and 17.8 moles of silica, leaving a 65.3 mole residual of kaolinite, quartz, Fe oxides, and refractory minerals. In weight units, the dissolved loss is 1.6 kg with a 3.66 kg residual. For complete weathering to gibbsite the values are 16.9, 36.3, and 46.8 moles, 2.7 and 2.55 kg. Thus, the penetration rates of the front into the rock are factors of 3.3 (kaolinite) and 1.9 (gibbsite) greater than the denudation rates calculated from the dissolved flux. Since the dissolved and suspended load transports contribute about equally to the denudation, the penetration rate of the front is several tens of meters per million years. The growth rate of the lateritic mantle against mechanical erosion is then about

TABLE 9 Weathering of Average Shield Rocks

Average Shield	mol%	Final Clay	Gibbsite	Kaolinite
Na+	6.62		6.62 aq	6.62 aq
K+	3.67		3.67 "	3.67 "
Mg+	2.49		2.49 "	2.49 "
Ca+	4.09		4.09 "	4.09 "
Si total	59.1		-	-
Si quartz	22.8		22.8	22.8
Si(OH)4 aq	-		36.3	17.8
Al mineral	18.5		-	18.5
Al(OH)3	-		18.5	-

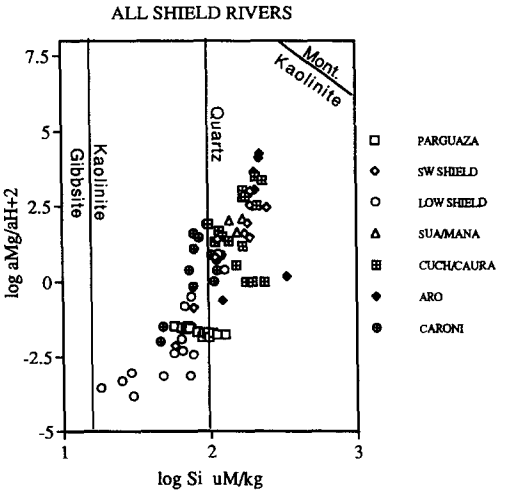

FIG. 14. Portion of the Mg-Si stability diagram illustrating that all the data fall in the stability field for kaolinite with the Lowland Shield data trending towards gibbsite. *Data used in this calculation are not corrected for the addition of sea salt.* Including this correction shifts the data points downwards slightly but not out of the kaolinite stability field.

half this value. Thus, the accumulation of one hundred meters of laterite takes on the order of ten million years. This calculation does not take into account the loss of Al to solution as $Al(OH)_3$ or other more complex species, nor does it allow for the attenuating and smoothing effect of solifluction processes or for differential penetration along fractured zones etc. Since the flux of water through the reaction front probably decreases with the increasing thickness of the residual mantle while mechanical erosion is relatively insensitive to this increase, there is probably a limit to the aereal thickness to which the mantle can accumulate. Based on the examples in Twidale (1982), this appears to be about 100 meters, although with much deeper accumulations locally along zones of weakness in the basement. Where the Si-alkali relationship extrapolates to the origin, it is likely that gibbsite is being formed directly at the reaction front. As the Si:[Na + K] ratio decreases the Si intercept becomes increasingly positive. This rotation in the Si/[Na + K] trend from a single to two end-members suggests an initial reaction to kaolinite with continued slower release of Si as gibbsite is formed higher in the section above the front.

7. CONCLUSIONS

From the conventional viewpoint, environmental conditions on the Guayana Shield are strongly conducive to rapid weathering. The elevations are substantial, temperatures are tropical at low and intermediate altitudes, rainfall is high and is strongly seasonal over much of the area, and there is an extensive cover of dense forest with minor savanna. Yet the denudation rates are low, averaging about ten meters per million years. The fluvial transport of dissolved and suspended material is approximately equal on a weight basis; however, the dominant component in the dissolved load is silica with ratios $Si:TZ^+$ ranging between 1.5 and 3. The generalized picture of weathering processes, implicitly derived from average river compositions (Holland, 1978; Meybeck, 1979, 1987), clearly does not apply.

On this tectonically quiescent Shield the relationship between elevation and weathering yield is not pronounced. The highlands have rates of between 15 and 20 m/m.y., the lowlands around 5 m/m.y. This compares with variations well in excess of a factor of ten between active margins and their foreland basins. In general, therefore, elevation per se is not the determining variable but, rather, the mechanism by which it is produced (Molnar and England, 1990), i.e., whether the elevation mechanism also generates relief. The eastern Shield underwent passive uplift associated with the opening of the Atlantic (Sidder and Mendoza, 1991). Recent examples of such uplift, e.g., in East Africa, are aseismic, save along the Rift valleys. Away from these features, there is little increase in the exposure of fresh surfaces or in local topographic gradients. Uplift does cause incision of stream channels, but at slow rates in basement rocks and with a small effect on exposure areas. In active margins, uplift is accompanied by extensive large scale faulting. This leads to dramatic increases in local relief, very steep slopes, and a continual production of fresh surfaces. The high hydraulic energy causes the rapid removal of unconsolidated material produced by partial weathering of the labile matrix minerals, the Na and Ca-feldspars. Local isostatic adjustment then increases relief even though the mean elevation of the range may be unchanged or even decrease (Molnar and England, 1990). The rates of denudation are limited solely by the rates of these processes, in the absence of glaciation which leads to even further acceleration.

On stable Shields, with low relief, chemical weathering is self-limiting, regardless of elevation. The subdued topography results in low hydraulic gradients. The dissolution reactions are incongruent and so a refractory residuum of quartz, kaolinite, gibbsite, and Fe oxides accumulates as a mantle. Solifluction in this cover tends to further smooth the topography. The site of primary weathering migrates vertically and a thin reaction front develops at depth (Twidale, 1990). While this is likely to be permanently waterlogged, the local flux of water is limited by the low permeability of the residual mantle. The flux of water through a given horizon in the profile probably decreases strongly with depth. Thus, the resultant measure of the weathering intensity, $Si:TZ^+$, increases with time as the relative importance to the fluvial flux of the transformation of kaolinite to gibbsite increases as compared to cation-producing processes going on at the stagnant reaction front. Such an evolution in the composition of the solid substrate is well reproduced in infiltration models (e.g., Lichtner, 1988). Since streams sample the whole profile, but differentially depending on the vertical gradient in permeability, equilibrium compositions are not to be expected in the resultant fluid mixture despite the overall consistency of the thermodynamic calculations (Fig. 14) with the interpretations based on the fluid chemistry alone.

The tendency of weathering to go to a limit is an intrinsic property of stable cratons in temperate and tropical climates. Disruption of the weathered mantle, in the absence of base level changes, can be caused only by the extension of solifluction to very low topographic gradients by the imposition of a freeze-thaw cycle (Mackay, 1993) or by the wholesale stripping of this material by glacial transport. This is consistent with the very old ages ascribed to the peneplanation surfaces of the stable cratons of the Southern hemisphere (King, 1962; Young, 1983; Twidale, 1990; Foster and Gleadow, 1993; Twidale and Campbell, 1993), which have generally been unaffected by any ice action. Over much of geologic time the Earth has been ice-free, with benign climates extending to high latitudes. Deeply mantled, weathered cratons, now restricted to tropical and southern latitudes, were likely the norm in the Northern Hemisphere. Inselberg forms, indicative of laterisation, have been identified in the Shield areas of continental Europe, southwest England and southeastern Greenland (Twidale, 1982). If located in the belts of high rainfall, as the Guayana Shield is now, these cratons would have been a strong source of dissolved silica, unaccompanied by a high cation and bicarbonate flux, as compared to the active margins. This may be the mechanism responsible for the enhanced deposition and preservation of biogenic opal in deep-sea sediments, as chert, that appears to be characteristic of pre-Oligocene times and is unaccompanied by significant changes in the carbonate compensation depth.

In a world where temperate climates extended to high latitudes the stable passive margins probably consisted in the main of cratonic blocks mantled either by shelf sequences of

platform carbonates, evaporites, sandstones, and shales or by a refractory weathering residuum. Topography, as at present, was related to the uplift associated with rifting or to the deeply eroded roots of previous mountain belts. In this situation the contribution of the platforms to the geochemical cycle would be restricted to recycled carbonates and evaporites from the platform cover and to silica from lateritic mantles developed over basement exposures. This is the situation today in the sedimentary basins and Shields of the Orinoco-Amazon system, most of Africa, Western Australia, and the great platforms drained by the Yangtze (Hu et al., 1982) and the rivers of eastern Siberia (Y. Huh and J. M. Edmond, unpubl. data). Very little "new" material is contributed with the exception of silica. The effect of their weathering on the global CO_2 system is small.

Since stable, peneplained continents are insignificant sources of new material, this can only come from tectonically active areas of continually renewed relief. These are of three types, all produced by plate motions; oceanic and continental active margins and Himalayan-type continental collision zones. The weathering of oceanic arcs probably produces a chemical signature similar to that from the low temperature alteration of oceanic crust. Andean-type continental arcs consist of uplifted platform sediments and associated basement rocks intruded by granitoids and capped by andesites. The rate of weathering of all these constituents is greatly accelerated as compared to their low-lying equivalents due to the tectonic and mechanical generation of relief (Stallard and Edmond, 1983, 1987) and, in extreme cases, glaciation. In addition, the transport of partially weathered detrital material to the flood plains behind the arc can produce severe weathering during seasonal inundation. This is clearly seen in the Llanos of the Orinoco (Johnsson et al., 1988) and is probably the norm in humid Tropical conditions (Hoffman and Grotzinger, 1993). The occurrence of oceanic vs. continental active margins is related to the age of the crust being subducted, with the transition taking place at about 50 m.y. (Molnar and Atwater, 1978; England and Wortel, 1980). Thus, Andean arcs should occur randomly in time with a greater probability of occurrence during periods of elevated spreading rates. Himalayan type collision causes the thermal reworking of basement rocks and their rapid elevation to great heights by thrust faulting followed by erosional and tectonic unroofing (Molnar, 1988; Harrison et al., 1992). Erosion is greatly accelerated by glacial processes. While the primary fluvial signal is strong (Sarin et al., 1989), again there is probably additional, more pervasive weathering during flood plain storage of the detritus (France-Lanord et al., 1993). The strontium isotope record in marine limestones is a proxy for Himalayan-style events (Edmond, 1992) and shows that they are random occurrences. Both collisional and Andean style tectonics affect a relatively small proportion of the continental area at any given time but are the loci of introduction of "new" aluminosilicate material and the net consumption of atmospheric CO_2.

General models of the geochemical cycle of the elements (e.g., Berner et al., 1983; Berner, 1994) focus on the level of atmospheric CO_2 as the driving agent of chemical weathering. The concept of a CO_2-temperature-weathering feedback is central (Walker et al., 1981). High CO_2 should lead, through the greenhouse effect, to high temperatures. These are assumed to accelerate weathering due to greater precipitation and resulting increased vegetative cover. This acceleration, in turn, draws down the atmospheric CO_2 producing a long-term stability. The model characterizes the weathering substrate only in terms of continental area (sea level), mean elevation, and the global proportion of rock types.

The arguments given above demonstrate that, to the contrary, specific tectonic events are the major driver of global weathering rates. Tectonics thus affects climate by causing the draw-down of atmospheric CO_2 (Ruddiman and Kutzbach, 1989; Raymo and Ruddiman, 1992). The events are random in time. The contemporary situation, large Andean and post-Andean margins in the Americas coupled with a major continental collision in Eurasia, perhaps represents an extreme. Certainly, the atmospheric CO_2 levels cannot be driven much lower without complete elimination of terrestrial vegetation. However, given the long persistence times of previous glacial epochs (Crowley, 1983), it appears that the present low pCO_2 levels can be maintained for tectonic timescales. Rather than being controlled by complex feedback mechanisms, the lower bound on atmospheric pCO_2 may constitute a kinetic minimum. The atmospheric He level, 5 ppmv, is controlled in this way. Its source, volcanic and metamorphic outgasing, is similar to that for CO_2; the sink is infinite, gravitational escape to space. The atmospheric level is maintained by the kinetic energy barrier to the achievement of thermal escape velocities. In the case of CO_2, adopting the first-order kinetic model of Lasaga (1980) and taking pCO_2 as a measure of the CO_2 reservoir available for reaction,

$$\frac{\partial[pCO_2]}{\partial t} = \varnothing - k \cdot A \cdot [pCO_2],$$

where $\varnothing$ is the volcanic/metamorphic input flux of CO_2, k is the weathering rate constant, and A is a dimensionless parameter, the effective weathering surface area normalised to the present, i.e., the contemporary value of A is unity. At steady state:

$$[pCO_2] = \frac{\varnothing}{k \cdot A}.$$

If $\varnothing$ and k are taken to be constant then pCO_2 depends only on A. In the present weathering regime, $A = 1$, the natural pCO_2 is ~280 ppmv. At small A, i.e., no recent active tectonics as, perhaps, in a supercontinent regime, $A \sim 0.1$, pCO_2 is ~10 times the present value; however, at large A, ~2, equivalent to the simultaneous collision of India *and* Australia with Southern Asia, pCO_2 is only half its present value, i.e., the current pCO_2 is close to the asymptote, effectively the kinetic minimum. In periods where most of the tectonic activity is oceanic, there is no well-defined constraint on the upper bound to pCO_2, if cratonic weathering processes are indeed self-limiting. This simple argument is given for illustrative purposes only and requires elaboration. As an alternative to the model formulations of Berner et al. (1983) and (Berner, 1994) and many others, however, it seems reasonable to consider active continental tectonics of Andean and Himalayan types as the major determinants on the atmospheric CO_2 levels.

Acknowledgments—A project of this magnitude obviously depended on the help of a large number of people. The Proyecto Orinoco-Apure was sponsored by the Ministerio del Ambiente y do los Recursos Naturales Renovables (MARNR) and the C. V. G. Electification del Caroni C. A. (EDELCA). The latter supported most of the logistics in the Caroni Basin. The Proyecto was coordinated by Abel Mejia in cooperation with Herman Roo (EDELCA) and C. Nordin and R. H. Meade of the USGS. We are especially grateful to the latter two for providing us with a unique opportunity to work on the Orinoco. The technical personnel of the Proyecto and of the USGS provided unstinting assistance and support in the field under unusually arduous conditions; the Proyecto generously covered all field expenses. For the large amount of laboratory work and for the coagulation and organization of the data, especial thanks are due to M. Khadem, S. Filler, and N. Adanya. We thank Professor S. Hart for very generous access to his mass spectrometers at MIT. Support to the MIT group for the laboratory work and for travel to Venezuela was provided by the Earth Surface Processes and Marine Chemistry Sections of the National Science Foundation.

Editorial handling: G. Rich Holdren Jr.

REFERENCES

Andreae M. O., Talbot R. W., Berresheim H., and Beecher K. M. (1990) Precipitation chemistry in central Amazonia. *J. Geophys. Res.* **95,** 16,987–16,999.

Berner R. A. (1994) GEOCARB II: a revised model of atmospheric CO_2 over Phanerozoic time. *Amer. J. Sci.* **294,** 56–91.

Berner E. K. and Berner R. A. (1987) *The Global Water Cycle.* Prentice-Hall.

Berner R. A., Lasaga A. C., and Garrels R. M. (1983) The carbonate-silicate cycle and its effect on atmospheric carbon dioxide over the past 100 million years. *Amer. J. Sci.* **283,** 641–683.

Briceño H. O. and Schubert C. (1990) Geomorphology of the Gran Sabana, Guayana Shield, southeastern Venezuela. *Geomorphol.* **3,** 125–141.

Briceño H., Schubert C., and Paolini J. (1991) Table-mountain geology and surficial geochemistry: Chimanta Massif, Venezuelan Guayana Shield. *J. South Amer. Earth Sci.* **3,** 179–194.

Brown E. T. et al. (1992) Beryllium isotope geochemistry in tropical river basins. *Geochim. Cosmochim. Acta* **56,** 1607–1624.

Brown E. T., Stallard R. F., Raisbeck G. M., and Yiou F. (1992) Determination of the denudation of Mount Roraima, Venezuela using cosmogenic ^{10}Be and ^{26}Al. *EOS* **73,** 170 (abstr.).

Brown E. T. et al. (1994) The development of iron crust lateritic systems in Burkina Faso, West Africa examined with in-situ—produced cosmogenic nuclides. *Earth Planet. Sci. Lett.* **124,** 19–33.

Chalcraft D. and Pye K. (1984) Humid tropical weathering of quartzite in southeastern Venezuela. *Z. Geomorph.* **28,** 321–332.

Clapperton C. M. (1993a) Nature of environmental changes in South America at the last glacial maximum. *Paleogeog. Paleoclim. Paleoecol.* **101,** 189–208.

Clapperton C. (1993b) *Quaternary Geology and Geomorphology of South America.* Elsevier.

Colodner D. et al. (1993) The geochemical cycle of rhenium: A reconnaissance. *Earth Planet. Sci. Lett.* **117,** 205–221.

Crowley T. J. (1983) The geologic record of climate changes. *Rev. Geophys. Space Phys.* **21,** 828–877.

Dougan T. W. (1977) The Imataca Complex near Cerro Bolivar, Venezuela: A calc-alkaline Archean protolith. *PreCamb. Res.* **4,** 237–268.

Edmond J. M. (1970) High precision determination of titration alkalinity and total carbon dioxide content of sea water by potentiometric titration. *Deep-Sea Res.* **17,** 737–750.

Edmond J. M. (1992) Himalayan tectonics, weathering processes and the strontium isotope record in marine limestones. *Science* **258,** 1594–1597.

England P. and Wortel R. (1980) Some consequences of the subduction of young slabs. *Earth Planet. Sci. Lett.* **47,** 403–415.

Foster D. A. and Gleadow A. J. W. (1993) Episodic denudation in East Africa: A legacy of intracontinental tectonism. *Geophys. Res. Lett.* **20,** 2395–2398.

France-Lanord C., Derry L., and Michard A. (1993) Evolution of the Himalaya since Miocene time: Isotopic and sedimentologic evidence from the Bengal Fan. In *Himalayan Tectonics* (ed. P. J. Treloar and M. Searle); *Geol. Soc. Lond. Spec. Pub. No. 74.*

Gac J. Y. (1980) Géochimie du bassin du Lac Tchad. Bilan de l'altération, de l'érosion et de la sédimentation. *Travaux et Documents OSTROM* **123,** 1–125.

Galloway J. M., Likens G. E., Keene W. C., and Miller J. M. (1982) The composition of precipitation in remote areas of the world. *J. Geophys. Res.* **87,** 8771–8786.

Garrels R. M. and Mackenzie F. T. (1971) *Evolution of Sedimentary Rocks.* Norton.

Gaudette H. E. and Olszewski W. J. (1985) Geochronology of the basement rocks, Amazonas Territory, Venezuela and the tectonic evolution of the western Guayana Shield. *Geol. Mijnb.* **64,** 131–143.

Gaudette H. E., Mendoza V., Hurley P. M., and Fairbairn H. W. (1978) Geology and age of the Parguaza rapakivi granite, Venezuela. *GSA Bull.* **89,** 1335–1340.

Gibbs A. K. and Barron C. N. (1983) The Guayana Shield reviewed. *Episodes,* 7–14.

Gibbs A. K. and Barron C. N. (1993) *The Geology of the Guiana Shield; Oxford Monog. Geol. Geophys. No. 22.*

Gibbs A. K. and Olszewski W. J. (1982) Zircon U-Pb ages of Guayana greenstone-gneiss terrane. *PreCamb. Res.* **17,** 199–214.

Gibbs A. K., Montgomery C. W., O'Day P. A., and Erslev E. A. (1986) The Archean-Proterozoic transition: evidence from the geochemistry of metasedimentary rocks of Guayana and Montana. *Geochim. Cosmochim. Acta* **50,** 2125–2142.

Gilbert G. K. (1917) Hydraulic-mining debris in the Sierra Nevada. *USGS Prof. Paper 105.*

Gong G. and Xu J. (1987) Environmental effects of human activities on rivers in the Huanghe-Huaihe-Haihe plain, China. *Geograf. Anal.* **69,** 181–188.

Gruau G., Martin H., Leveque B., and Capdevila R. (1985) Rb-Sr and Sm-Nd geochronology of Lower Proterozoic granite-greenstone terranes in French Guayana, South America. *PreCamb. Res.* **30,** 63–80.

Harrison T. M., Copeland P., Kidd W. S. F., and Yin A. (1992) Raising Tibet. *Science* **255,** 1663–1670.

Hoffman P. F. and Grotzinger J. P. (1993) Orographic precipitation, erosional unloading and tectonic style. *Geology* **21,** 195–198.

Holland H. D. (1978) *The Chemistry of the Atmosphere and Ocean.* Wiley.

Hu M. H., Stallard R. F., and Edmond J. M. (1982) Major ion chemistry of some large Chinese rivers. *Nature* **298,** 550–553.

Johnsson M. J. (1990) Overlooked sedimentary particles from tropical weathering environments. *Geology* **18,** 107–110.

Johnsson M. J., Stallard R. F., and Meade R. H. (1988) First-cycle quartz arenites in the Orinoco River basin, Venezuela and Colombia. *J. Geol.* **96,** 263–277.

Kalliokoski J. (1965) Geology of the north-central Guayana Shield. *GSA Bull.* **76,** 1027–1050.

King L. C. (1962) *The Morphology of the Earth.* Oliver and Boyd.

Klinkhammer G. P. and Chan L. H. (1990) Determination of barium in marine waters by isotope dilution inductively coupled plasma mass spectrometry. *Anal. Chim. Acta* **232,** 323–329.

Lasaga A. C. (1980) The kinetic treatment of geochemical cycles. *Geochim. Cosmochim. Acta* **44,** 815–828.

Lee D. S., Edmond J. M., and Bruland K. W. (1986) Bismuth in the Atlantic and North Pacific: A natural analogue for plutonium and lead? *Earth Planet. Sci. Lett.* **76,** 254–262.

Lewis W. M. and Weibezahn F. (1981) The chemistry and phytoplankton of the Orinoco and Caroni rivers, Venezuela. *Arch. Hydrobiol.* **91,** 521–528.

Lewis W. J., Saunders J. F., Levine S. N., and Wiebezahn F. H. (1986) Organic carbon in the Caura River, Venezuela. *Limnol. Oceanog.* **31,** 653–656.

Lewis W. M., Hamilton S. K., Jones S. L., and Runnels D. D. (1987) Major element chemistry, weathering and element yields for the Caura River drainage, Venezuela. *Biogeochem.* **4,** 159–181.

Lichtner P. C. (1988) The quasi-stationary state approximation to coupled mass transport and fluid-rock interaction in a porous medium. *Geochim. Cosmochim. Acta* **52,** 143–165.

Lopez E. C. and Bisque R. E. (1975) Study of the weathering of basic, intermediate and acidic rocks under humid tropical conditions. *Colo. School Mines, Quart.* **40,** 209–217.

Mackay J. R. (1993) Air temperature, snow cover, creep of frozen ground, and the time of ice-wedge cracking, western Arctic coast. *Can. J. Earth Sci.* **30,** 1720–1729.

McKee E. D. (1989) The Waters and Sediments of the Rio Orinoco and its Major Tributaries, Venezuela and Colombia, Chapter B, Sedimentary structures and textures of Rio Orinoco channel sands, Venezuela and Colombia. *USGS Water-Supply Paper* **2326B,** B1–B23.

Meade R. H. (1969) Errors in using modern stream-load data to estimate natural rates of denudation. *GSA Bull.* **80,** 1265–1274.

Meade R. H. (1988) Movement and storage of sediment in river systems. In *Physical and Chemical Weathering in Geochemical Cycles* (ed. A. Lerman and M. Meybeck); *NATO ASI Series C-Vol 251,* pp. 165–179.

Meade R. H. (1994) Suspended sediments of the modern Amazon and Orinoco rivers. *Quat. Intl.* (in press).

Meade R. H., Weibezahn F. H., Lewis W. M., and Pérez Hernández D. (1990a) Suspended-sediment budget for the Orinoco River. In *The Orinoco River as an Ecosystem* (ed. F. H. Weibezhan et al.), pp. 55–79. Impresos Rubel CA, Caracas.

Meade R. H., Yuzyk T. R., and Day T. J. (1990b) Movement and storage of sediment in rivers of the United States and Canada. In *The Geology of North America,* Vol. O-1; *Surface Water Hydrology, GSA,* pp. 255–280.

Measures C. I. and Edmond J. M. (1983) The geochemical cycle of ^{9}Be: A reconnaissance. *Earth Planet. Sci. Lett.* **66,** 101–110.

Menard H. W. (1961) Some rates of regional erosion. *J. Geol.* **69,** 154–160.

Meybeck M. (1979) Concentrations des eaux fluviales en elements majeurs et apports en solution aux oceans. *Rev. Geol. Dyn. Geog. Phys.* **21,** 215–246.

Meybeck M. (1987) Global chemical weathering from surficial rocks estimated from river dissolved loads. *Amer. J. Sci.* **287,** 401–428.

Meyer H. O. A. and McCallum M. E. (1993) Diamonds and their sources in the Venezuelan portion of the Guyana Shield. *Econ. Geol.* **88,** 989–998.

Milliman J. D. and Meade R. H. (1983) World-wide delivery of river sediment to the oceans. *J. Geol.* **91,** 1–21.

Molnar P. (1988) A review of the geophysical constraints on the deep structure of the Tibetan Plateau, the Himalaya and the Karakoram, and their tectonic implications. *Phil. Trans. Roy. Soc. London* **A326,** 33–88.

Molnar P. and Atwater T. (1978) Interarc spreading and Cordilleran tectonics as alternates related to the age of subducted oceanic lithosphere. *Earth Planet. Sci. Lett.* **41,** 330–340.

Molnar P. and England P. (1990) Late Cenozoic uplift of mountain ranges and global climate change: chicken or egg? *Nature* **346,** 29–34.

Montes R., San Jose J. J., Garcia-Miragaya J., and Parra N. (1985) pH of bulk precipitation during 3 consecutive annual courses in the Trachypogon savannas of the Orinoco Llanos, Venezuela. *Tellus* **37B,** 304–307.

Montgomery C. W. (1979) Uranium-lead geochronology of the Archean Imataca Series, Venezuelan Guayana Shield. *Contrib. Mineral. Petrol.* **69,** 167–176.

Montgomery C. W. and Hurley P. M. (1978) Total-rock U-Pb and Rb-Sr systematics in the Imataca Series, Guayana Shield, Venezuela. *Earth Planet. Sci. Lett.* **39,** 281–290.

Murnane R. J. and Stallard R. F. (1990) Germanium and silicon in rivers of the Orinoco drainage basin. *Nature* **344,** 749–752.

Négrel P., Allègre C. J., Dupré B., and Lewin E. (1993) Erosion sources determined by inversion of major and trace element ratios and strontium isotope ratios in river water; the Congo Basin case. *Earth Planet. Sci. Lett.* **120,** 59–76.

Newton R. M., Weintraub J., and April R. (1987) The relationship between surface water chemistry and geology in the North Branch of the Moose River. *Biogeochem.* **3,** 21–35.

Nixon P. H., Davies G. R., Rex D. C., and Gray A. (1992) Venezuela kimberlites. *J. Volcanol. Geotherm. Res.* **50,** 101–115.

Nordin C. F. (1985) The sediment load of rivers. In *Facets of Hydrology,* Vol. 2 (ed. J. C. Rodda), pp. 183–204. Wiley.

Nordin C. F. and Meade R. H. (1980) The flux of organic carbon to the oceans; some hydrological considerations. In *Flux of Organic Carbon by Rivers to the Oceans; U.S.D.O.E. CONF 8009140 UC-11,* pp. 173–218.

Nordin C. F. and Perez-Hernandez D. (1989) *The Waters and Sediments of the Rio Orinoco and its Major Tributaries, Venezuela and Colombia,* Chap. A, *Sand waves, bars and wind-blown sands of the Rio Orinoco, Venezuela and Colombia, USGS Water-Supply Paper 2326A,* A1–A74.

Onstott T. C., Hall C. M., and York D. (1989) ^{40}Ar/^{39}Ar thermochronometry of the Imataca complex, Venezuela. *PreCamb. Res.* **42,** 255–291.

Palmer M. R. and Edmond J. M. (1989) The strontium isotope budget of the modern ocean. *Earth Planet. Sci. Lett.* **92,** 11–26.

Palmer M. R. and Edmond J. M. (1992) Controls over the strontium isotopic composition of river water. *Geochim. Cosmochim. Acta* **56,** 2099–2112.

Palmer M. R. and Edmond J. M. (1993) Uranium in river water. *Geochim. Cosmochim. Acta* **57,** 4947–4955.

Priem H. N. A., Boelrijk N. A. I. M., Hebeda E. H., Verdurmen E. A. Th., and Verschure R. H. (1971) Isotopic ages of the Trans-Amazonian acidic magmatism and the Nickerie Metamorphic Episode in the PreCambrian basement of Suriname, South America. *GSA Bull.* **82,** 1667–1680.

Priem H. N. A., Boelrijk N. A. I. M., Hebeda E. H., Verdurmen E. A. Th., and Verschure R. H. (1973) Age of the PreCambrian Roraima Formation in northeastern South America: Evidence from isotopic dating of Roraima pyroclastic volcanic rocks in Suriname. *GSA Bull.* **84,** 1677–1684.

Priem H. N. A. et al. (1982) Geochronology of the PreCambrian in the Amazonas region of southeastern Colombia (Western Guayana Shield). *Geol. Mijnb.* **61,** 229–242.

Raymo M. E. and Ruddiman W. F. (1992) Tectonic forcing of late Cenozoic climate. *Nature* **359,** 117–122.

Reeder S. W., Hitchon B., and Levinson A. A. (1972) Hydrochemistry of the surface waters of the Mackenzie River drainage basin, Canada, I, Factors controlling the inorganic composition. *Geochim. Cosmochim. Acta* **36,** 825–866.

Reid A. R. and Bisque R. E. (1975) Stratigraphy of the diamond-bearing Roraima Group, Estado Bolivar, Venezuela. *Colo. School Mines, Quart.* **70,** 61–82.

Richter F. M., Rowley D. B., and DePaolo D. J. (1992) Sr isotopic evolution of seawater: The role of tectonics. *Earth Planet. Sci. Lett.* **109,** 11–24.

Rogers J. J. W. et al. (1984) Early poststabilisation sedimentation and later growth of shields. *Geol.* **12,** 607–609.

Ruddiman W. F. and Kutzbach J. E. (1989) Forcing of late Cenozoic Northern Hemisphere climate by plateau uplift in Southern Asia and the American West. *J. Geophys. Res.* **94,** 18,409–18,427.

Sarin M. M., Krishnaswami S., Dilli K., Somayajulu B. L. K., and Moore W. S. (1989) Major ion chemistry of the Ganga-Brahmaputra river system: Weathering processes and fluxes to the Bay of Bengal. *Geochim. Cosmochim. Acta* **53,** 997–1009.

Saunders I. and Young A. (1983) Rates of surface processes on slopes, slope retreat and denudation. *Earth Surf. Proc. Landforms* **8,** 473–501.

Savage K. M. and Potter P. E. (1991) Petrology of modern sands of the Rios Guaviare and Inirida, Southern Colombia: tropical climate and sand composition. *J. Geol.* **99,** 289–298.

Schorin H. and Puchelt H. (1987) Geochemistry of a ferruginous bauxite from southeast Venezuela. *Chem. Geol.* **64,** 127–142.

Schumm S. A. (1963) *The Disparity between Present Rates of Denudation and Orogeny; USGS Prof. Paper 454-H.*

Shoemaker E. M. et al. (1990) Ages of Australian meteorite craters—a preliminary report. *Meteoritics* **25,** 409.

Sidder G. B. (1990) *Mineral Occurrences of the Guiana Shield, Venezuela; USGS, Open-File Report 90-16.*

Sidder G. B. and Martinez F. (1990) *Geology, Geochemistry and Mineral Resources of the Upper Caura River Area, Bolivar State, Venezuela; USGS Open-File Report 90-231.*

Sidder G. B. and Mendoza S. V. (1991) *Geology of the Venezuelan Guayana Shield and its Relation to the Entire Guayana Shield; USGS Open-File Rept. 91-141.*

Snelling N. J. and McConnell R. B. (1969) The geochronology of Guayana. *Geol. Mijnb.* **48,** 201–213.

Stallard R. F. (1980) Major Element Chemistry of the Amazon River System. Ph.D. dissertation, MIT/WHOI.

Stallard R. F. (1987) Cross-channel mixing and its effect on sedimentation in the Orinoco river. *Water Resour. Res.* **23,** 1977–1986.

Stallard R. F. and Edmond J. M. (1981) Geochemistry of the Amazon I. Precipitation chemistry and the marine contribution to the dissolved load at the time of peak discharge. *J. Geophys. Res.* **86,** 9844–9858.

Stallard R. F. and Edmond J. M. (1983) Geochemistry of the Amazon 2. The influence of geology and weathering environment on the dissolved load. *J. Geophys. Res.* **88,** 9671–9688.

Stallard R. F. and Edmond J. M. (1987) Geochemistry of the Amazon 3. Weathering chemistry and limits to dissolved inputs. *J. Geophys. Res.* **92,** 8293–8302.

Tan F. C. and Edmond J. M. (1993) Carbon isotope geochemistry of the Orinoco Basin. *Estuar. Coast. Shelf Sci.* **36,** 541–547.

Trimble S. W. (1977) The fallacy of stream equilibrium in contemporary denudation studies. *Amer. J. Sci.* **277,** 876–887.

Twidale C. R. (1982) *Granite Landforms.* Elsevier.

Twidale C. R. (1990) The origin and implications of some erosional landforms. *J. Geol.* **98,** 343–364.

Twidale C. R. and Campbell E. M. (1993) Remnants of Gondwana in the Australian landscape. In *Gondwana Eight* (ed. R. H. Findlay et al.), pp. 573–583. Balkema.

USGS (1993) *Geology and Mineral Resource Assessment of the Venezuelan Guayana Shield. USGS Bull. 2062.*

Vegas-Vilarrubia T., Paolini J., and Herrera R. (1988). A physicochemical survey of blackwater rivers from the Orinoco and Amazon basins in Venezuela. *Archiv fur Hydrobiol.* **111,** 491–506.

Walker J. C. G., Hays P. B., and Kasting J. F. (1981) A negative feedback mechanism for the long-term stabilization of Earth's surface temperature. *J. Geophys. Res.* **86,** 9776–9782.

Wedepohl K. H. (1969) Composition and abundance of common igneous rocks. In *Handbook of Geochemistry* (ed. K. H. Wedepohl), Vol 1, Chap. 7, pp. 227–249. Springer-Verlag.

Weibezahn F. H. (1985) Concentraciones de especies quiímicas disueltas y transporte de sólidos suspendidos en el alto y medio Orinoco y sus variaciones estacionales (Febrero 1984–Febrero 1985). *Univ. Simón Bolívar Inst. Recursos Naturales, Proyecto Estudio Preliminar del Río Orinoco como Sistema Ecológico (PECOR).*

Weibezahn F. H. (1990) Hidroquiímica y sólidos suspendidos en el alto y medio Orinoco. In *The Orinoco River as an Ecosystem* (ed. F. H. Weibezahn et al.), pp. 151–210. Impresos Rubel CA, Caracas.

Yee H. S., Measures C. I., and Edmond J. M. (1987) Selenium in the tributaries of the Orinoco in Venezuela. *Nature* **326,** 686–689.

Young R. W. (1983) The tempo of geomorphological change: Evidence from southeastern Australia. *J. Geol.* **91,** 221–230.